Radboud University Nijmegen

Faculty of Science
High Energy Physics

Calculating Love numbers using black hole perturbation theory

Characterizing the effects of external fields on black holes

Master Thesis Physics & Astronomy
Specialization Particle- and Astrophysics

Author:
Joost Remie

Supervisor:
dr. B.P. Bonga

Second reader:
dr. F.S. Saueressig

September 2021

Abstract

Despite their rigidity, both the shape and gravitational field of black holes are affected by external bodies. The effects of the external bodies are conveniently characterized by surficial and gravitational Love numbers. In this thesis, these Love numbers are calculated for various spherically symmetric and therefore relatively simple black holes. The calculations will be carried out using black hole perturbation theory that will be applied to the black holes described by the Schwarzschild and Reissner-Nordström metric. To be confident about the results, the calculations will be carried out in both the popular Regge-Wheeler gauge and the more physically motivated light cone gauge.

Acknowledgements

This thesis has been written in a strange, difficult and uncertain time caused by the corona virus. When the pandemic started, I was quite scared to get the virus and become ill. Due to that and the fact that I had to work from home, I was struggling to concentrate on my studies. Furthermore, it was rather strange to do a master internship at the High Energy Physics department without ever physically being at the department. Also, I have only talked to my supervisor Béatrice Bonga through Zoom for more than a year.

Despite that, every conversation I had with Béatrice was enjoyable as well as helpful. Not only did she help me whenever I got stuck during my research, but when I was having a difficult time and having trouble focussing or I thought I was not making enough progress with my research, I felt comfortable to tell Béatrice about that too. We also talked about things that were not about the research. Something that stuck with me is that we talked about what I was going to do after I graduated and I told her I was considering becoming a teacher. Then she told me that her brother is also a teacher and that he really likes it and she named some disadvantages as well.

Therefore, I would like to thank Béatrice for her patience and understanding, for giving me the opportunity to do research under her guidance and for the pleasant conversations. I have learned a lot and not exclusively about physics but especially the physics was very challenging and interesting. Also, I would like to thank Frank Saueressig for agreeing to be the second reader and hope he will enjoy reading this thesis.

Contents

Chapter 1

Introduction

1.1 Motivation

While you are reading this the earth is steadily moving along its orbit around the sun and also spinning around its (tilted) axis. At the same time, the moon is revolving around the earth and as it does its surface is deformed by the gravitational field of the earth. How the surface of the moon is deformed depends on where the moon is on its orbit, as is schematically shown in figure 1.1.

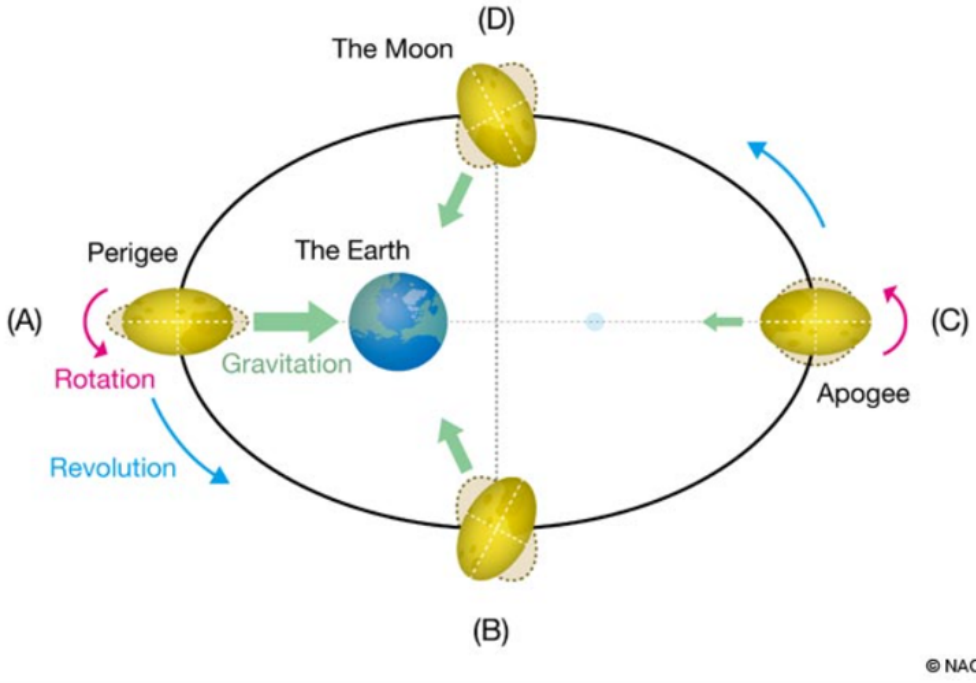

Figure 1.1: The shape of the surface of the moon as it moves on its elliptic orbit around the earth.

Even though the mass of the earth is much larger than the mass of the moon, the shape of the earth is also affected by the moon. It is being deformed as its mass distribution is constantly changing due to the fact that a large portion of the earth's mass is in liquid form and can therefore more easily be displaced, resulting in the tides. This displacement of water is due to gravitational force that the moon exerts as it rotates around the earth. So even though the moon has a considerably lower mass than the earth, it can still have a notable effect on the earth.

Something similar happens to black holes as they occupy a part of space that contains all kinds of other massive objects as well. Black holes are strongly curved regions of spacetime, where gravity is so strong that any matter within the event horizon can never escape the gravitational pull. This leads to the fact that black holes are very rigid objects, meaning that it is very difficult to deform them. Naturally, the extremely strong gravitational field of a black hole will affect other bodies in space by deforming them. However it is not impossible for black holes to be deformed by external objects. Hence, the shape of the black hole will in turn be affected by the other massive objects it deforms.

The goal of this thesis is to characterize some of the different ways in which a black hole can be deformed. For example, its surface can be deformed due to an external gravitational potential in a similar way to how the surface of the earth is deformed by the gravitational force of the moon. However, it will turn out that the surface of a black hole is not the only thing that is affected by an external field.

1.2 Overview

This thesis is structured in the following way: First, some important properties of black holes and how they can be described mathematically in different coordinate systems and gauges will be introduced. Then it will be explained how perturbation theory can be applied to black holes in general and how the gauge conditions of two gauges that are common in literature, the light cone gauge and the Regge-Wheeler gauge, can be expressed in terms of restrictions on the components of the metric perturbation.

Then, perturbation theory will be applied to two different black holes. First, it will be applied to an uncharged, nonrotating black hole that is described by the Schwarzschild metric. This will describe how a black hole and its gravitational field are affected by an external gravitational field. Next, perturbation theory is applied to a charged, nonrotating black hole described by the Reissner-Nordström metric. In this case, the black hole itself (and possibly the perturbing body (or bodies)) will be charged, leading not only to a perturbation of the gravitational potential but a perturbation of the electromagnetic potential as well. Expressions describing all these perturbations will be found by demanding that the full metric obeys Einstein's equations and in the case of a charged black hole Maxwell's equations as well.

Once the perturbations are known, they can be used to calculate the Love numbers corresponding to each deformation. Love numbers are dimensionless quantities that characterize the deformation of astronomical objects under the influence of external forces. To determine these Love numbers, many expressions will be expanded in terms of multipole moments. It will turn out that an external gravitational field not only affects the surface of a black hole by deforming it, but it will also induce gravitational multipole moments in the gravitational field far away from the black hole. Furthermore, an external electromagnetic field will displace the charge distribution on the surface of a charged black hole and in addition it will induce electromagnetic multipole moments of the electromagnetic field far away from the black hole. Each of these different effects of external fields can be characterized by different Love numbers.

In the appendix, the Newman-Penrose and Geroch-Held-Penrose formalism are introduced that can also be used to describe black hole perturbation theory. They are formalisms that are not derived from any specific coordinate system and are particularly convenient because they represent a compact way of writing the relevant equations. This is especially useful to describe perturbation theory applied to a rotating black hole described by the Kerr metric, which in a coordinate formulation would lead to quite complicated equations that are difficult to solve. Due to lack of time the formalism will not be used for this purpose in this thesis, but some calculations that were done for the Schwarzschild and Reissner-Nordström metrics will be repeated, to show their compactness.

Chapter 2

Theory

In this section, some properties of black holes and a technique called black hole perturbation theory will be introduced. Furthermore, coordinate transformations and gauge transformations will be described, that will feature in the rest of the text. Also, two different gauges that will be used, the light cone gauge and the Regge-Wheeler gauge, are introduced. Then, black hole Love numbers will be defined, that can be calculated by means of black hole perturbation theory.

2.1 Black holes

General Relativity is a theory that describes gravity as a property of spacetime. It is a generalization of Special Relativity and it describes the relation between the curvature and the energy-momentum content of spacetime by means of the Einstein field equations:

$$R_{\mu\nu} - \frac{1}{2} g_{\mu\nu} R = \frac{8\pi G}{c^4} T_{\mu\nu}. \tag{2.1.1}$$

In this system of differential equations, $g_{\mu\nu}$ is the spacetime metric, $R_{\mu\nu}$ the Ricci curvature tensor, R the Ricci curvature scalar and $T_{\mu\nu}$ the energy-momentum tensor. From now on, geometrized units will be used such that Newton's constant G and the speed of light c are set to 1. In short, the energy-momentum content leads to curvature of spacetime, which in turn gives rise to gravity.

The fact that their gravity is so strong makes black holes very rigid, it is hard to deform their perfectly spherical shape. Any external gravitational force will in general be small compared to the gravity of the black hole, making the situation suitable for perturbation theory, which will be introduced soon. Black holes are interesting objects for applying and testing the theory of General Relativity, as the physics of some unperturbed black holes is already described quite well by the corresponding metric.

2.1.1 The Schwarzschild metric

The metric provides a mathematical description of black holes that represents a solution to Einstein's equations. The simplest black hole is an uncharged, nonrotating one that is described by the Schwarzschild metric. This is one of the very few exact solutions to Einstein's equations or more precisely, to the vacuum Einstein equations, as the region outside an uncharged, stationary black hole can be treated as a vacuum. In spherical coordinates, see section 2.3, the Schwarzschild metric is:

$$g_{\mu\nu} dx^\mu dx^\nu = -f(r) dt^2 + \frac{1}{f(r)} dr^2 + r^2 (d\theta^2 + \sin\theta^2 d\phi^2). \tag{2.1.2}$$

with in this case $f(r) = 1 - \frac{2M}{r}$.

In these coordinates it is clear that the center of the black hole at $r = 0$ is a singularity as $1/r$ diverges there. However, in these coordinates there is another singularity at the Schwarzschild radius $r = 2M$, where $1/f(r)$ diverges. It turns out that the latter singularity is a coordinate singularity as it can be removed by moving to a different coordinate system, as will be shown later. The three-dimensional surface of the black hole at the position $r = 2M$ is called the (event) horizon.

2.1.2 The Reissner-Nordström metric

A slightly more complicated black hole is a charged, nonrotating one that is described by the Reissner-Nordström metric. In spherical coordinates it looks the same as the Schwarzschild metric, only now $f(r) = 1 - \frac{2M}{r} + \frac{Q^2}{r^2}$.

In this case, the center of the black hole is still a singularity, as expected. However, there are now two values of r where $1/f(r)$ diverges. These values are determined by setting $f(r) = 0$, which results in an inner horizon at $r_- = M - \sqrt{M^2 - Q^2}$ and an outer horizon at $r_+ = M + \sqrt{M^2 - Q^2}$. The outer horizon plays the role of the event horizon that was encountered for a Schwarzschild black hole, it marks the outer limit of the black hole and the location of the surface. The function $f(r)$ will appear in many of the equations in this thesis. For brevity, it will therefore be denoted as f from now on.

Having two horizons is something a Reissner-Nordström black hole has in common with a Kerr black hole, which is an uncharged but rotating black hole. The Kerr metric is considerably more complicated and it is much more difficult to solve the resulting equations. However, it is more interesting to investigate a Kerr black hole since it is closer to an actual, physical black hole. The fact that a Reissner-Nordström black hole also has two horizons while its metric is less complicated, makes it a good alternative to investigate the effects of two horizons.

2.2 Black hole perturbation theory

Perturbation theory is an important technique that is widely used in many branches of physics and other sciences. It is a mathematical method for finding approximate solutions to problems that cannot be solved exactly. It involves perturbing an exact solution, which means that the exact solution will be used as a background to which a perturbation will be added. In this thesis, perturbation theory will be applied to black holes. Specifically it will be applied to uncharged and charged nonrotating black holes.

2.2.1 Perturbing the metric

It is only interesting to investigate deformed black holes as an isolated Schwarzschild black hole will remain at a fixed position in spacetime, maintaining its original size and mass. Fortunately, a physical black hole is located in space, where other objects reside that also generate a gravitational field. The field of any external object will perturb the gravitational field and therefore the metric of the black hole. Assuming the deviation from the original metric is small, it is quite natural to use perturbation theory to describe the metric after the perturbation.

In this thesis, black hole perturbation theory will be used to study the deformation of different black holes in the presence of an external tidal field. The external tidal field will be described as a perturbation of the metric of the black hole under consideration. Black hole perturbation theory can be written in a general way as:

$$g_{\alpha\beta} = \overline{g}_{\alpha\beta} + \varepsilon p^{(1)}_{\alpha\beta} + \varepsilon^2 p^{(2)}_{\alpha\beta} + O[\varepsilon^3], \tag{2.2.1}$$

where ε is a small constant, $g_{\alpha\beta}$ is the full metric, $\overline{g}_{\alpha\beta}$ is the background metric and the $p^{(i)}_{\alpha\beta}$ describe the i-th order of the perturbation. In this thesis, only perturbing terms of linear order (that is, proportional to

ε) will be taken into consideration.

2.2.2 Expansion of the perturbation

The perturbation of a spherically symmetric metric can be decomposed into scalar, vectorial and tensorial spherical harmonics. The scalar harmonics are the standard spherical harmonics $Y_{lm}(\theta, \phi)$ satisfying the eigenvalue equation $[\Omega^{AB} D_A D_B + l(l+1)]Y^{lm} = 0$, where $\Omega_{AB} = \text{diag}(1, \sin^2\theta)$ is the metric of a two-sphere and D_A is the covariant derivative compatible with this metric. Of the vectorial as well as tensorial harmonics, there are two types, one with even parity and one with odd parity. The even-parity spherical harmonics are defined as $Y^{lm}_A := D_A Y^{lm}$ and the odd-parity ones are $X^{lm}_A := -\varepsilon^B_A D_B Y^{lm}$. For the tensorial spherical harmonics, the even-parity part can be split into a trace and traceless part. Specifically, the trace part is given by $\Omega_{AB} Y^{lm}$ and the traceless part by Y^{lm}_{AB} with:

$$Y^{lm}_{AB} := [D_A D_B + \frac{1}{2} l(l+1)\Omega_{AB}]Y^{lm}. \tag{2.2.2}$$

The odd-parity tensor harmonics are:

$$X^{lm}_{AB} := -\frac{1}{2}(\varepsilon^C_A D_B . + \varepsilon^C_B D_A) D_C Y^{lm}. \tag{2.2.3}$$

The parity of a vectorial or tensorial harmonic determines how it behaves under a parity transformation. An even-parity harmonic is even under a parity transformation, i.e. it remains unchanged, whereas an odd-parity harmonic picks up a minus sign [1].

2.2.3 Even-parity sector

The metric perturbation can thus be split into a part with even parity and a part with odd parity, corresponding to the component of the perturbation that can be expanded in terms of the even- and odd-parity spherical harmonics respectively. Only the even-parity sector will be taken into consideration in the rest of this thesis. Next, the following notation as used in [1] will be introduced for the temporal-radial, angular and mixed terms of the metric respectively: $g_{ab} = \overline{g}_{ab} + p_{ab}\varepsilon$, $g_{AB} = r^2\Omega_{AB} + p_{AB}\varepsilon$ and $g_{aB} = p_{aB}\varepsilon$. Here, lower case Latin indices run over 0 and 1, thus g_{ab} refers to the (t, r)-part of the metric whereas the upper-case Latin indices take the values 2 and 3, referring to the angular part. Greek indices will run over all components, from 0 to 4. The perturbation terms that appear in this notation are:

$$p_{ab} = \sum_{lm} h^{lm}_{ab}(t, r) Y^{lm}(\theta, \phi) \tag{2.2.4a}$$

$$p_{aB} = \sum_{lm} j^{lm}_a(t, r) Y^{lm}_B \tag{2.2.4b}$$

$$p_{AB} = r^2 \sum_{lm} (K^{lm}(t, r)\Omega_{AB} Y^{lm} + G^{lm}(t, r) Y^{lm}_{AB}), \tag{2.2.4c}$$

where the sum runs over the multipole moments denoted by l and m takes values from $-l$ to l.

As a further simplification, only the quadrupole terms ($l = 2$) of the multipole expansions will be taken into account in all upcoming calculations. Furthermore, only situations in which the time dependence is irrelevant will be considered: time dependence is sufficiently slow such that the tidal forces never take the body out of equilibrium. In other words, the external time scale is much longer than the internal time scale related to the body's internal processes. Therefore, we are in the static tides regime [2].

2.3 Coordinate transformations

Since the metric (including possible perturbations) is a tensor, it is by definition independent of the choice of coordinates. Therefore, there is a freedom to choose a coordinate system that is convenient for a specific situation. Also, a coordinate transformation from one coordinate system to another can always be found.

2.3.1 Spherical coordinates

The most obvious coordinates system is the spherical one, exploiting the exact spherical symmetry of an unperturbed black hole. Then, the Schwarzschild metric will be described by t, r, θ and ϕ which is how it was denoted in the introduction. An advantage of this coordinate system is that the metric is diagonal.

Although this might be the most concise way of writing the Schwarzschild metric, there are reasons why another coordinate system would be preferable. One of these reasons is that a coordinate singularity appears at $r = 2M$ when the metric is written in this way. When $r = 2M$, f becomes zero, which is a problem in the rr-component of the metric, where f appears in the denominator. To see that this is indeed a coordinate singularity and not a physical singularity, one can refer to a different coordinate system and see that the singularity does not appear there.

2.3.2 Eddington-Finkelstein coordinates

A coordinate system that is commonly used to remove this coordinate singularity is the Eddington-Finkelstein coordinate system. Here, radial light rays are used to define surfaces of constant time. In this case, the advanced-time coordinate v is used instead of t: $v = t + r + 2M\ln(r/2M - 1)$. From this relation follows that: $dt = dv - \frac{dr}{f}$, which results in:

$$ds^2 = -f dv^2 + 2dvdr + r^2 d\theta^2 + r^2 \sin^2\theta d\phi^2 \tag{2.3.1}$$

Here, v is called the advanced time (since terms are added to t) coordinate, which is constant on incoming light cones. The coordinate r is an affine parameter, meaning that it depends linearly on proper time. The angular coordinates θ and ϕ are constant along generators of light cones [3].

By writing the metric this way, there is no term where f appears in the denominator, therefore setting $r = 2M$ no longer gives rise to a singularity. In fact, the range of r is now $r \in (0, \infty)$, the condition $r > 2M$ is no longer required. Hence, the interior (where $r < 2M$) of the black hole can also be described in this coordinate system. However, there is also a disadvantage of this particular coordinate system, which is that the metric contains off-diagonal terms.

2.3.3 General coordinate transformation

Under a general transformation from one coordinate system x^μ to another $x^{\mu'}$, the metric tensor transforms as:

$$g_{\mu'\nu'} = \frac{\partial x^\mu}{\partial x^{\mu'}} \frac{\partial x^\nu}{\partial x^{\nu'}} g_{\mu\nu}. \tag{2.3.2}$$

As an example, this will be used to transform from Eddington-Finkelstein to general spherical coordinates. Using $dv = dt + f^{-1}dr$ and the relevant metric components in the former coordinate system: $g_{vv} = -f$,

$g_{vr} = g_{rv} = 1$ and $g_{rr} = 0$, one arrives at:

$$\begin{aligned}
g_{tt} &= \left(\frac{\partial v}{\partial t}\right)^2 g_{vv} + 2\frac{\partial v}{\partial t}\frac{\partial r}{\partial t}g_{vr} + \left(\frac{\partial r}{\partial t}\right)^2 g_{rr} \\
&= 1^2 \cdot (-f) + 2 \cdot 1 \cdot 0 \cdot 1 + 0^2 \cdot 0 = -f \\
g_{tr} &= \frac{\partial v}{\partial t}\frac{\partial v}{\partial r}g_{vv} + \frac{\partial v}{\partial t}\frac{\partial r}{\partial r}g_{vr} + \frac{\partial r}{\partial t}\frac{\partial v}{\partial r}g_{rv} + \frac{\partial r}{\partial t}\frac{\partial r}{\partial r}g_{rr} \\
&= 1 \cdot (\frac{1}{f}) \cdot (-f) + 1 \cdot 1 \cdot 1 + 0 \cdot (\frac{1}{f}) \cdot 1 + 0 \cdot 1 \cdot 0 = 0 \\
g_{rr} &= \left(\frac{\partial v}{\partial r}\right)^2 g_{vv} + 2\frac{\partial v}{\partial r}\frac{\partial r}{\partial r}g_{vr} + \left(\frac{\partial r}{\partial r}\right)^2 g_{rr} \\
&= (\frac{1}{f})^2 \cdot (-f) + 2(\frac{1}{f}) \cdot 1 \cdot 1 + 1^2 \cdot 0 = \frac{1}{f}
\end{aligned}$$

This results in the desired Schwarzschild metric.

2.4 Gauge freedom

It has been shown that the perturbation of a black hole can be expanded in terms of spherical harmonics of even- and odd parity. Performing this expansion effectively leads to a separation of variables, dividing the perturbation into one part containing the angular dependence and another part containing the radial dependence (neglecting time dependence). The radial dependence is what the next part will focus on and it turns out there is a certain amount of freedom in this dependence. This is a manifestation of gauge freedom, meaning that the physics that is described is independent of the choice of gauge. Therefore, there is a freedom to choose a particular gauge, which will be exploited in this thesis.

2.4.1 Gauge transformations

Another way to explain gauge freedom is that there is freedom to perform a gauge transformation, after which many expressions will look quite differently, but nevertheless they will still be describing the same physical situation. A general gauge transformation is given by:

$$p_{\mu\nu} \to p'_{\mu\nu} = p_{\mu\nu} - \nabla_\mu \xi_\nu - \nabla_\nu \xi_\mu. \tag{2.4.1}$$

Here, ∇_μ is the covariant derivative operator compatible with the background metric.

Even-parity gauge transformations are generated by a dual vector field $\Xi_\alpha = (\Xi_a, \Xi_A)$ which can also be expanded in terms of (only scalar and vectorial) spherical harmonics:

$$\Xi_a = \xi_a^{lm}(r) Y^{lm}(\theta^A) \tag{2.4.2}$$

$$\Xi_A = \xi^{lm}(r) Y_A^{lm}(\theta^A) \tag{2.4.3}$$

The functions ξ, ξ_v, and ξ_r capture the r-dependence of the gauge transformation [3].

This gauge freedom (or part of it) can be removed by choosing a particular gauge, which places restrictions on the metric perturbation. Two common ones in the field of black hole perturbation theory are the light cone and Regge-Wheeler gauge, which will be discussed separately.

2.4.2 Light cone gauge

A commonly used gauge in black hole perturbation theory is the light cone gauge. It is convenient to describe it in Eddington-Finkelstein coordinates because they have a clear geometrical meaning that is preserved in

the light cone gauge. There is only one property of the coordinates that is not preserved in the light cone gauge, which is that of r as an areal radius.

The preservation of the geometrical meaning of the coordinates is ensured by specific conditions that the light cone gauge places on the metric. These gauge conditions are generated by the null vector: $l_\alpha := -\nabla_\alpha v = (-1, 0, 0, 0)$ and (raising indices with the metric in Eddington-Finkelstein coordinates) $l^\alpha = (0, -1, 0, 0)$. The metric can be used to raise (or lower) the index of this null vector: $l_\alpha = g_{\alpha\beta} l^\beta$. Writing the metric as the sum of the background metric and a linear perturbation term and demanding that $l_\alpha = (-1, 0, 0, 0)$ continues to hold for $l_\alpha = (\overline{g}_{\alpha\beta} + p_{\alpha\beta}) l^\beta$ leads to the condition: $p_{\alpha r} = 0$. Four gauge conditions result from this:

$$p_{vr} = p_{rr} = p_{rA} = 0 \tag{2.4.4}$$

These gauge conditions are relatively simple algebraic conditions, which is another advantage of the light cone gauge [3].

It is important to note that, choosing a specific gauge does not necessarily fix the gauge completely, there may be residual gauge freedom. In that case, there are specific functions generating a gauge transformation that can be added to the perturbation. Adding these functions will still alter some of the expressions but the components of the perturbation will continue to obey the light cone gauge conditions. In particular, the light cone gauge conditions are obeyed as long as the ξ_v, ξ_r and ξ satisfy:

$$\frac{\partial \xi_v}{\partial r} + \frac{\partial \xi_r}{\partial v} + \frac{2M}{r^2}\xi_r = 0 \tag{2.4.5a}$$

$$\frac{\partial \xi_r}{\partial r} = 0 \tag{2.4.5b}$$

$$\frac{\partial \xi}{\partial r} + \xi_r - \frac{2}{r}\xi = 0 \tag{2.4.5c}$$

These equations are obeyed by the functions:

$$\xi_v = -af + b \tag{2.4.6a}$$

$$\xi_r = a \tag{2.4.6b}$$

$$\xi = ar + cr^2, \tag{2.4.6c}$$

where a, b and c are arbitrary constants. This means that in the light cone gauge the functions generating the gauge transformation need not be identically zero. There is still some freedom to change the functions describing the metric perturbation, while keeping them within the light cone gauge. This residual gauge freedom changes the components of the perturbation in the following way:

$$h_{vv} \to h'_{vv} = h_{vv} + \frac{2M}{r^2} b \tag{2.4.7a}$$

$$j_v \to j'_v = j_v + af - b \tag{2.4.7b}$$

$$K \to K' = K + \frac{6}{r}a - \frac{2}{r}b + 6c \tag{2.4.7c}$$

$$G \to G' = G - \frac{2}{r}a - 2c. \tag{2.4.7d}$$

The components that are not listed here do not change [3].

2.4.3 Regge-Wheeler gauge

Despite the advantages of the light cone gauge, it is not the gauge that is used most frequently in literature on black hole perturbation theory, the Regge-Wheeler gauge is. While it does not preserve the geometrical

meaning of the coordinates, nor lead to asymptotically-flat solutions far away from the perturbation, the equations describing the perturbations are simpler than in the light cone gauge.

The Regge-Wheeler gauge conditions are:

$$t^a p_{ab} = 0 = t^a p_{aB}, \tag{2.4.8}$$

where t^a is the timelike Killing vector of the Schwarzschild spacetime: $t^a = -\varepsilon^{ab} r_b$. In the coordinates used here, this Killing vector is: $t^a = (1, 0)$. Writing out the above equation, the Regge-Wheeler gauge conditions, again for the even-parity sector are: $j_a = 0 = G$. Another disadvantage of the Regge-Wheeler gauge is that it effectively sets the transverse trace-free part of the perturbations to zero ($G = 0$), making it hard to extract any gravitational radiation information [4].

In terms of the expansions of the perturbation in terms of scalar, vectorial and tensorial harmonics, the Regge-Wheeler gauge conditions can be written as: $j_v = j_r = G = 0$. Let us investigate if this leaves any residual gauge freedom, as was the case in the light cone gauge. For that, equations (4.6)-(4.9) of Martel Poisson will be used. To stay within the Regge-Wheeler gauge, first of all we must have: $G' = G = 0$, and therefore $\xi = 0$. Furthermore, $j'_v = j_v$ and hence: $\xi_v + \nabla_v \xi = 0 \Rightarrow \xi_v = 0$. The same with $j'_r = j_r$ leads to $\xi_r = 0$. Hence, there is no residual gauge freedom in the Regge-Wheeler gauge.

Part of the Regge-Wheeler gauge conditions can be denoted by setting specific component of the metric perturbation to zero. Writing it in a similar way as was done for the light cone gauge leads to:

$$p_{vA} = p_{rA} = 0. \tag{2.4.9}$$

In addition, the Regge-Wheeler gauge conditions set the traceless part of the angular part of the metric perturbation to zero.

2.5 Love numbers

The goal of this thesis is to describe how certain black holes are deformed under the influence of external fields. To describe such deformations, the Love numbers of the black holes will be calculated. These are dimensionless quantities characterizing the deformation of astronomical objects under the influence of external forces. Essentially, Love numbers capture how difficult it is to deform a black hole. Whether the shape of the surface is deformed or the gravitational potential is perturbed, there is a Love number to quantify it. Hence, there are multiple types of Love numbers, also depending on the type of black hole under consideration.

First, the two most general Love numbers are defined that can be calculated for any black hole. An external gravitational field can lead to a deformation of the surface of the black hole, but it will also affect the gravitational field of the black hole. The quantities characterizing such deformations will simply be called Love numbers here.

When the bodies that give rise to external fields are charged, they will also produce an electromagnetic field. Such a field can affect the charge distribution on the surface of the black hole. Furthermore, if the black hole is also charged, its electromagnetic field will be perturbed by the external one. The effects of an electromagnetic field on a black hole are characterized by what will be called electromagnetic susceptibilities which can be thought of as "electromagnetic Love numbers".

In this thesis, only the quadrupole Love numbers will be calculated. However, the definitions will be given in terms of the full multipole expansions and only when specific values are calculated we will restrict ourselves to the quadrupole part, setting $l = 2$.

2.5.1 Surficial Love numbers

The following definition of surficial Love numbers is convenient since a relativistic generalization is quite apparent due to its tensorial (and thus coordinate-invariant) formulation. The deformation of the initially spherical surface of the body can be translated into a change in the intrinsic curvature of the surface. This intrinsic curvature is represented by the two dimensional Ricci scalar $\mathcal{R}$ that can be derived from the metric on the deformed surface (which is two dimensional), which is to first order in the surface displacement: $ds^2 = R^2(1 + 2\delta R/R)d\Omega^2$. The corresponding perturbed Ricci scalar, again to first order, is then:

$$\mathcal{R} = \frac{1}{R^2}(2 + \delta\mathcal{R}), \tag{2.5.1}$$

where $\delta\mathcal{R}$ is the change of the Ricci scalar describing the intrinsic curvature of the original, spherical surface and R is the radial position of the surface (for Schwarzschild: $R = 2M$). The surficial Love numbers h_l then feature in the spherical-harmonic decomposition of this perturbation of the Ricci scalar:

$$\delta\mathcal{R} = -2\sum_{l=2}^{\infty} \frac{l+2}{l} h_l \frac{R^{l+1}}{M} \mathcal{E}_L(\theta, \phi)\Omega^L. \tag{2.5.2}$$

where L is a multi-index containing l individual indices, $L = a_1a_2...a_l$ and l again labels the different multipole terms. Hence, there are many different surficial Love numbers, one for every l. Recalling that the external field that gives rise to this multipole perturbation of the Ricci scalar can also be expanded into multipole moments the surficial Love number can then be defined as: The dimensionless ratio between the l-th multipolar component of the deformation and the l-th multipolar component of the external gravitational potential [2].

2.5.2 Gravitational Love numbers

The gravitational Love numbers are defined far away from the black hole, in the far-field regime. It turns out that the gravitational Love numbers actually come in two guises: an electric-type gravitational Love number that is associated with the gravito-electric part of the tidal gravitational field and a magnetic one associated with the gravito-magnetic part. To describe gravitational Love numbers, the tidal field as well as the multipole moment of a mass distribution must be characterized [5].

By comparing the Newtonian potential with the weak-field limit of the vv-component of the perturbed metric, the latter can be written in terms of the effective potential as: $g_{vv} = -(1 - 2U)$. The gravitational potential from classical mechanics can thus be written in terms of a component of the metric which is a general relativistic quantity: $U = \frac{1}{2}(g_{vv} + 1)$. When the spherical body is embedded in the external gravitational potential produced by the remote bodies, the total potential can be written as:

$$U(x) = -\sum_{l=2}^{\infty} \frac{(l-2)!}{l!} x^L \mathcal{E}_L + \frac{M}{r} + \sum_{l=2}^{\infty} \frac{(2l-1)!!}{l!} \frac{n^L I_L}{r^{l+1}}, \tag{2.5.3}$$

where L is again a multi-index and I_L are the induced mass multipole moments. The first sum captures the applied l-pole tidal field, whereas the second sum corresponds to the induced l-pole moment and the M/r term in the middle represents the Newtonian potential of the black hole itself.

Since we are dealing with a weak and slowly varying external tidal field, the induced multipole moments are proportional to the external, applied multipoles. The constant of proportionality involves the tidal love number k_l:

$$I_L = -\frac{2(l-2)!}{(2l-1)!!} k_l R^{2l+1} \mathcal{E}_L. \tag{2.5.4}$$

This can be used to express the gravitational potential in the following way:

$$U = \frac{M}{r} - \sum_{l=2}^{\infty} \frac{(l-2)!}{l!} n^L \mathcal{E}_L r^l \left[1 + 2k_l (R/r)^{2l+1}\right]. \tag{2.5.5}$$

To remove the multi-index L and make the notation more intuitive, the field $n^L\mathcal{E}_L$ can be expanded in terms of spherical harmonics that we have encountered before in this thesis. Such an expansion is given by:

$$n^L(\theta,\phi)\mathcal{E}_L = \sum_{m=-l}^{l} \mathcal{E}_{lm} Y_{lm}(\theta,\phi) \qquad \text{with} \qquad \mathcal{E}_{lm} = \oint_S n^L \overline{Y}_{lm} d\Omega \tag{2.5.6}$$

Finally, the full gravitational potential then reads [6]:

$$U = \frac{M}{r} - \sum_{lm} \frac{(l-2)!}{l!} \mathcal{E}_{lm} r^l \left[1 + 2k_l \left(\frac{R}{r}\right)^{2l+1}\right] Y_{lm}(\theta,\phi). \tag{2.5.7}$$

In this expression, the Newtonian potential of the black hole itself with mass M can be identified, as well as the external potential defined in the previous section. The additional term, proportional to k_l denotes the (gravitational) multipole moment that is induced in the black hole. The dimensionless proportionality constants k_l are in fact the gravitational Love numbers, of which there again exists one for every multipole term, thus for every l. The exact definition for gravitational Love numbers is then: the dimensionless ratio of the l-th multipolar component of the body's induced gravitational potential and the l-th multipolar component of the external gravitational field [7].

2.5.3 Electromagnetic surficial Love numbers

The electromagnetic surficial Love numbers characterize how the charge distribution on the surface of the black hole is distorted by an external body. Figure 2.5.3 provides a sketch of the situtation: on the left is the situation before introducing external bodies, where the charge of the black hole is evenly distributed over its surface. Once an external body that is also charged is introduced, the charge will be pushed more to one side of the black hole.

Figure 2.1: The surface charge distribution without (left) and with (right) and external body.

Recall that polarizability is the tendency of matter to acquire a multipole moment when subjected to an external field. More precisely, the polarizability of an object is the constant of proportionality between the external field and the multipole moment induced by this field in the body under consideration. Hence, gravitational Love numbers can alternatively be called gravitational polarizability [8].

The reason for making an analogy between Love numbers and polarizability is that there are multiple similarities between the two. The total gravitational potential outside the body under consideration is made up of the potential caused by the body itself, the external field and the field induced in the body (or the body's response). Similarly, the total polarization is a combination of any frozen-in polarization, the original field causing the polarization and the new field induced by the external field.

The electromagnetic surficial Love numbers describing the effect of external bodies on the electromagnetic field of the black hole are in fact the polarizability of the black hole. The deformation of the charge distribution on the surface leads to a polarization of the black hole, the size of which depends on the external field and these electromagnetic surficial Love numbers.

The value of these Love numbers can be extracted from the surface charge density on the outer horizon:

$$\sigma = \frac{1}{4\pi}\left[\frac{\partial A_0(r)}{\partial r}\right]_{r=M+\sqrt{M^2-Q^2}},$$

where A_0 is the zeroth component of the electromagnetic potential A_μ. How the electromagnetic surficial Love numbers h_l^{EM} can be extracted from this is explained in [8].

The angular part of A_0 can be expanded expanded into spherical harmonics $P_l(\cos\theta)$ to obtain:

$$A_0(r) = \sum_{l=0}^{\infty} \tau_l g_l(r) P_l(\cos\theta), \tag{2.5.8}$$

where the τ_l are the electric analogs of the tidal coefficients introduced in [8]. Similarly, for σ the following expansion can be made:

$$\sigma = \sum_{l=1}^{\infty} \sigma_l P_l(\cos\theta). \tag{2.5.9}$$

Then, the h_l^{EM} can be extracted from:

$$4\pi R\sigma_l = h_l^{EM}\tau_l R^l, \tag{2.5.10}$$

with $R = M + \sqrt{M^2 - Q^2}$.

2.5.4 Electromagnetic far-field Love numbers

The electromagnetic far-field Love numbers are defined in the same way as the gravitational Love numbers, only the former are not related to the gravitational potential but to the electromagnetic potential. Therefore, a multipole expansion must be made of the zeroth component of the electromagnetic potential (A_0) instead of the 00-component of the metric (through $U = -\frac{1}{2}(g_{vv} + 1)$). These Love numbers are again defined far away from the black hole, hence far-field. The definition of the electromagnetic far-field Love numbers is: the dimensionless ratio of the l-th multipolar component of the body's induced electromagnetic potential and the l-th multipolar component of the external electromagnetic field.

2.5.5 Overview of Love numbers

In this section, all types of Love numbers that can be defined for a Schwarzschild and a Reissner-Nordström black hole are summarized in a table. For a Schwarzschild black hole there are two kinds, the surficial and gravitational ones. For a Reissner-Nordström black hole, these two kinds can also be defined and in addition the electromagnetic surficial and far-field Love numbers can be defined. Each cell in the table briefly describes what the corresponding Love number characterizes.

Love number/black hole type	Schwarzschild	Reissner-Nordström
Surficial	Surface deformation	Surface deformation
Gravitational	Induced grav. multipole moment	Induced grav. multipole moment
Electromagnetic surficial	X	Distorted charge distribution
Electromagnetic far-field	X	Induced e.m. multipole moment

In the table, grav. is an abbreviation for gravitational and e.m. for electromagnetic.

Chapter 3

Black holes in an external tidal field

Now some specific applications of black hole perturbation theory will be considered. The discussion will feature neutral and charged black holes, both of which will be investigated in the Regge-Wheeler as well as the light cone gauge. Everything will be described in terms of Eddington-Finkelstein coordinates, unless mentioned otherwise.

3.1 The background

For both black holes that will be considered, the following notation for line element of the background metric will be used:

$$ds^2 = g_{ab}dx^a dx^b + r^2\Omega_{AB}d\theta^A d\theta^B \tag{3.1.1}$$

where lower-case Latin indices run over 0 and 1 (t, r) and the capital indices run over 2 and 3 (the angular part, θ and ϕ). The second, angular part will be the same for the uncharged and charged black hole, whereas the first part will differ in both cases.

3.2 Charged black hole in Regge-Wheeler gauge

The procedure will be described in an order different to how it was carried out. Actually, perturbation theory was first applied to the Schwarzschild black hole in both gauges. That is because the equations arising from perturbation theory are simpler in this case, making it more convenient to become familiar with black hole perturbation theory. The reason that the description will be in a different order, is that the Schwarzschild expressions are supposed to follow from the $Q \to 0$ limit of the Reissner-Nordström expressions, which will be checked later.

For this reason, only perturbation theory applied to a Reissner-Nordström black hole will be described in detail here. The procedure will be repeated twice, once in the Regge-Wheeler and once in light cone gauge. The Regge-Wheeler gauge will be discussed first since the equations resulting from the corresponding gauge conditions are simpler in this gauge.

3.2.1 Metric perturbation

Using the conditions for the Regge-Wheeler gauge as given in section 2.4.3, the non-zero components of the perturbed metric tensor up to second order are, as defined in ref. [1]:

$$g_{tt} = -f + fH_0(r)\mathcal{E}^q(\theta,\phi)\varepsilon + O[\varepsilon]^2 \tag{3.2.1a}$$
$$g_{tr} = H_1(r)\mathcal{E}^q(\theta,\phi)\varepsilon + O[\varepsilon]^2 \tag{3.2.1b}$$
$$g_{rr} = \frac{1}{f} + \frac{H_2(r)}{f}\mathcal{E}^q(\theta,\phi)\varepsilon + O[\varepsilon]^2 \tag{3.2.1c}$$
$$g_{AB} = r^2K(r)\Omega_{AB}\mathcal{E}^q(\theta,\phi)\varepsilon + O[\varepsilon]^2. \tag{3.2.1d}$$

Here, $\mathcal{E}^q(\theta,\phi)$ captures the angular dependence which can be expanded in terms of spherical harmonics. The functions that are to be determined in this case are $H_0(r)$, $H_1(r)$, $H_2(r)$, $K(r)$, that capture the radial dependence of the perturbation. These functions were originally defined in the (t, r, θ, ϕ)-coordinates but since Eddington-Finkelstein coordinates will be used here, a transformation must be performed, leading to:

$$g_{vv} = -f + fH_0(r)\mathcal{E}^q(\theta,\phi)\varepsilon + O[\varepsilon]^2 \tag{3.2.2a}$$
$$g_{vr} = 1 + (H_1(r) - H_0(r))\mathcal{E}^q(\theta,\phi)\varepsilon + O[\varepsilon]^2 \tag{3.2.2b}$$
$$g_{rr} = \frac{H_0(r) - H_1(r) + H_2(r)}{f}\mathcal{E}^q(\theta,\phi)\varepsilon + O[\varepsilon]^2 \tag{3.2.2c}$$
$$g_{AB} = r^2K(r)\Omega_{AB}\mathcal{E}^q(\theta,\phi)\varepsilon + O[\varepsilon]^2. \tag{3.2.2d}$$

3.2.2 The stress-energy tensor

In the linearized Einstein field equations, the perturbed Einstein tensor will feature on the left-hand side. For the right-hand side, the linearized stress-energy tensor must be determined. To do this, the electromagnetic vector potential including a perturbation will be used as a starting point. In (t, r, θ, ϕ)-coordinates the vector potential is: $A_\mu = (-Q/r, 0, 0, 0)$ which will also have to be transformed to Eddington-Finkelstein coordinates to obtain: $A_\mu = (-Q/r, Q/(fr), 0, 0)$.

The electromagnetic tensor can be calculated from this using the formula:

$$F_{\mu\nu} = 2\partial_{(\mu}A_{\nu)} = \partial_\mu A_\nu - \partial_\nu A_\mu. \tag{3.2.3}$$

However, just like the metric, the vector potential also has to be perturbed. The perturbation can be written as:

$$\delta A_\mu = \left(\frac{u_1(r)}{r}\mathcal{E}^q(\theta,\phi), \frac{(u_2(r) - u_1(r))}{f(r)r}\mathcal{E}^q(\theta,\phi), u_3(r)\mathcal{E}^q_\theta(\theta,\phi), u_3(r)\mathcal{E}^q_\phi(\theta,\phi)\right), \tag{3.2.4}$$

which is already in the right coordinates and introduces three additional unknown functions $u_1(r)$, $u_2(r)$ and $u_3(r)$. This perturbation leads to a perturbation in the electromagnetic tensor, which in turn leads to a perturbed stress-energy tensor.

With the conventions that are being used in this thesis, the full expression for the stress energy tensor is:

$$T_{\mu\nu} = \frac{1}{4\pi}\left(F_\mu{}^\alpha F_{\nu\alpha} - \frac{1}{4}g_{\mu\nu}F^{\alpha\beta}F_{\alpha\beta}\right). \tag{3.2.5}$$

These expressions for the perturbed metric and stress-energy tensor can be plugged into Einstein's equations to obtain differential equations for the seven undetermined functions. Before listing all of the equations, the $\theta\phi$- and vr-component of Einstein's equations will be used: $\frac{1}{2}(-H_0(r) + H_2(r))\varepsilon + O[\varepsilon]^2 = 0$ and $-\frac{3H_1(r)\varepsilon}{r^2} + O[\varepsilon]^2 = 0$. Only using perturbation theory up to first order, the $O[\varepsilon]^2$ term can be set to zero which yields: $H_0(r) = H_2(r)$ and $H_1(r) = 0$. Hence, only five unknown functions $H_0(r)$, $K(r)$, $u_1(r)$, $u_2(r)$ and $u_3(r)$ remain, which means we also require that number of equations. The full set of equations can be found in Appendix A.

3.2.3 Additional constraints

In addition to Einstein's equations, Maxwell's equations must hold, providing additional constraints to determine the unknown functions. In terms of the electromagnetic tensor, Maxwell's equations are: $D^\mu F_{\mu\nu} = 0$. Here, D^μ is the covariant derivative compatible with the full, linearized metric $g_{\mu\nu}$. Another constraint can be derived from exploiting the gauge freedom in the electromagnetic sector by picking a convenient gauge. For example, the Lorenz gauge can be chosen, which entails the condition $D^\mu A_\mu = 0$. To avoid an abundance of equations, the full set of Maxwell's equations and the equation resulting from the gauge choice are also presented in Appendix A.

3.2.4 Undetermined functions

Here, only the equations that were used to find the functions $H_0(r)$, $K(r)$, $u_1(r)$, $u_2(r)$ and $u_3(r)$ will be listed. First of all, plugging $H_0(r) = H_2(r)$ and $H_1(r) = 0$ into the θ-component of Maxwell's equations and the Lorenz gauge provides two equations that only contain $u_2(r)$ and $u_3(r)$.

$$\frac{1}{r}\left((Q^2 r - 2Mr^2 + r^3)\frac{d^2u_3(r)}{dr^2} - 2r^2\frac{du_2(r)}{dr} + (2Mr - 2Q^2)\frac{du_3(r)}{dr} + 2ru_2(r)\right) = 0 \tag{3.2.6a}$$

$$r\frac{du_2(r)}{dr} + u_2(r) - 3u_3(r) = 0. \tag{3.2.6b}$$

With two equations and two unknowns, the equations can be solved to obtain expressions for $u_2(r)$ and $u_3(r)$. These have been solved using Maple which is generally better at solving differential equations than Mathematica. The above equations are solved by these expressions for $u_2(r)$ and $u_3(r)$ respectively:

$$\begin{aligned} u_2(r) = \frac{1}{r}\Bigg(K_2\Bigg((3Q^2M - 3Q^2r - 6M^2r + 9Mr^2 - 3r^3)\frac{1}{2}\left[\log\left(1 - \frac{M-r}{\sqrt{M^2-Q^2}}\right) - \log\left(1 + \frac{M-r}{\sqrt{M^2-Q^2}}\right)\right] \\ + (2Q^2 + M^2 - 6Mr + 3r^2)\sqrt{M^2-Q^2}\Bigg) + K_1\left(-Q^2M + Q^2r + 2M^2r - 3Mr^2 + r^3\right)\Bigg) \end{aligned} \tag{3.2.7a}$$

$$\begin{aligned} u_3(r) = K_2\Bigg((-2M^2 + 6Mr - Q^2 - 3r^2)\frac{1}{2}\left[\log\left(1 - \frac{M-r}{\sqrt{M^2-Q^2}}\right) - \log\left(1 + \frac{M-r}{\sqrt{M^2-Q^2}}\right)\right] \\ + 3(r-M)\sqrt{M^2-Q^2}\Bigg) + K_1\left(r^2 - 2Mr + \frac{1}{3}(Q^2 + 2M^2)\right)\Bigg) \end{aligned} \tag{3.2.7b}$$

These expressions contain two free parameters K_1 and K_2 that are dimensionless and independent of r. The parameters can still depend on a dimensionless combination of Q and M and this dependence will be determined later.

Two more components of Maxwell's equations and all of Einstein's equations remain to find expressions for $u_1(r)$, $H_0(r)$ and $K(r)$. To solve Einstein's equations, the $r\phi$-component of Einstein's equations was used first to express $K'(r)$ (where the prime indicates a derivative with respect to r) in terms of $u_1(r)$, $H_0(r)$ and derivatives thereof. Furthermore, the rr-component of Einstein's equations can be used to express $K(r)$ in terms of $u_1(r)$, $H_0(r)$ and derivatives thereof. Of course, the derivative of the latter expression must agree with the former expression. In other words, the difference between first expression and the derivative of the second is set to zero, which provides us with a new equation:

$$\begin{aligned} K(r) = &-\frac{Q^2 - Mr}{2r}\frac{dH_0(r)}{dr} - \frac{Q}{r}\frac{du_1(r)}{dr} \\ &+ \frac{Q^4 + Q^2r^2 + 2r^2(-M^2 - Mr + r^2)}{2r^2(Q^2 + r(-2M + r))}H_0(r) + \frac{Q^3 - Qr}{r^2(Q^2 + r(-2M + r))}u_1(r) \end{aligned} \tag{3.2.8}$$

This equation together with the v-component of Maxwell's equations with the expression for $\frac{dK(r)}{dr}$ plugged

in leads to two equations for the two unknowns $u_1(r)$ and $H_0(r)$:

$$\begin{aligned}
0 =& -\frac{Q^2 - Mr}{2r}\frac{d^2H_0(r)}{dr^2} - \frac{Q}{r}\frac{d^2u_1(r)}{dr^2} \\
&+ \frac{Q^4 - MQ^2 + Mr^2(-M+r)}{r^2(Q^2 + r(-2M+r))}\frac{dH_0(r)}{dr} + \frac{2(Q^3 - MQr)}{r^2(Q^2 + r(-2M+r))}\frac{du_1(r)}{dr} \\
&+ \frac{-Q^6 + 3MQ^4r + 3Q^2r^3(-2M+r) + Mr^3(-2M^2 + 6Mr - 3r^2)}{r^3(Q^2 + r(-2M+r))^2}H_0(r) \\
&- \frac{2Q(Q^4 + r^3(-3M+r) + Q^2r(-3M+4r))}{r^3(Q^2 + r(-2M+r))^2}u_1(r) \qquad (3.2.9a) \\
0 =& \frac{Q^2 - 2Mr + r^2}{r^3}\frac{d^2u_1(r)}{dr^2} + \frac{Q(Q^2r + (-2M+r))}{r^4}\frac{dH_0(r)}{dr} \\
&+ \frac{2(-Q^3 + MQr)}{r^5}H_0(r) + \frac{4Q^2 - 6r^2}{r^5}u_1(r) \qquad (3.2.9b)
\end{aligned}$$

The solutions of these equations can then be plugged into eq. (3.2.8) in terms of the these functions to find an expression for $K(r)$. The solutions of eqs. (3.2.9a), (3.2.9b) and (3.2.8) for $H_0(r)$, $u_1(r)$ and $K(r)$ are:

$$\begin{aligned}
H_0(r) =& C_{1a}\left(-\frac{M(Q^2 + r(-2M+r))}{r}\right) + C_{1b}\left(-\frac{(4M+r)(Q^2 + r(-2M+r))}{r}\right) \\
&+ C_2\Bigg(\frac{1}{r(Q^2 + r(-2M+r))}\Bigg(\sqrt{M^2+Q^2}(6M^4r + 5Q^4r + 3Q^2r^3 - 2M^3(Q^2 + 28r^2) \\
&+ M^2(49Q^2r + 57r^3) - M(13Q^4 + 34Q^2r^2 + 15r^4)) - \frac{3}{2}(4M^2 + Q^2 - 5Mr)(Q^2 + r(-2M+r)) \\
&\cdot\left[\log\left(1 - \frac{M-r}{\sqrt{M^2-Q^2}}\right) - \log\left(1 + \frac{M-r}{\sqrt{M^2-Q^2}}\right)\right]\Bigg)\Bigg) \qquad (3.2.10a) \\
K(r) =& C_{1a}\left(4M^2 - \frac{MQ^2}{r} - 3Mr\right) + C_{1b}\left(\frac{18M^2r - r(Q^2+r^2) - 4M(Q^2+3r^2)}{r}\right) \\
&+ C_2\Bigg(\sqrt{M^2+Q^2}(2M^3r + 13MQ^2 - 21M^2r - 9Q^2r + 15Mr^2) + \frac{3}{2}(6M^3r - 4M^2(Q^2+3r^2) \\
&- Q^2(Q^2+3r^2) + M(9Q^2r + 5r^3)) \cdot \left[\log\left(1 - \frac{M-r}{\sqrt{M^2-Q^2}}\right) - \log\left(1 + \frac{M-r}{\sqrt{M^2-Q^2}}\right)\right]\Bigg) \qquad (3.2.10b) \\
u_1(r) =& C_{1a}\left(-\frac{M(Q^2 + r(-2M+r))(Q^2 + r(-M+r))}{2Qr}\right) \\
&+ C_{1b}\left(-\frac{(Q^2 + r(-2M+r))(-4M^2r + Q^2r + 4M(Q^2+r^2))}{2Qr})\right) \\
&+ C_2\Bigg(\frac{1}{2Qr}\Bigg((M-Q)(M+Q)(4M^4r + 5Q^4r + 3Q^2r^3 - 2M^2(Q^2 + 12r^2) - M(13Q^4 + 21Q^2r^2) \\
&+ 12M^2(3Q^2r + r^3)) - \frac{3}{2}(-Q^2 + (2M-r)r)(4M^3r + 6MQ^2r - (4M^2 + Q^2)(Q^2 + r^2)) \\
&\cdot\left[\log\left(1 - \frac{M-r}{\sqrt{M^2-Q^2}}\right) - \log\left(1 + \frac{M-r}{\sqrt{M^2-Q^2}}\right)\right]\Bigg)\Bigg) \qquad (3.2.10c)
\end{aligned}$$

that involve the dimensionless constants C_{1a}, C_{1b} and C_2.

3.2.5 Behaviour of the Reissner-Nordström perturbation in the Regge-Wheeler gauge

This section contains plots of the two functions $H_0(r)$ and $K(r)$ describing the metric perturbation in the Regge-Wheeler gauge, as a function of the dimensionless variable r/M. Specifically, figure 3.1 and 3.2 show how the part of the solutions of $H_0(r)$ and $K(r)$ proportional to C_1 behave respectively. To make these plots, C_2 was set equal to zero and the two constants C_{1a} and C_{1b} were combined into the constant C_1 in the following way: $C_{1a} = -4C_{1b} = C_1$. Why this particular combination was chosen will be explained later. The functions that will be plotted are the following:

$$H_0(r) = -\frac{Q^2 - 2Mr + r^2}{M^2} C_1 \tag{3.2.11a}$$

$$K(r) = 2 - \frac{Q^2 + r^2}{M^2} C_1 \tag{3.2.11b}$$

Each plot contains multiple lines, with each line corresponding to a different value of Q, from 0 to very close to M.

First consider the effect that the charge of the black hole has on the part of the perturbation given by eq. (3.2.11a). From a cosmological perspective, the scale of the plot is quite small, only from the center of the singularity to about five times radial distance of the horizon (where it would be for a Schwarzschild black hole). Hence, any differences between the different lines should be particularly evident given that the effect of the charge Q is larger for smaller r. Despite that, the different lines representing plots of $H_0(r/M)$ for different values of Q almost completely overlap. This means that the behaviour of this part of the perturbation is barely (if at all) affected by a change of the charge of the black hole.

Next, consider the behaviour as a function of r/M: As r/M increases, corresponding to a displacement away from the black hole, the plot becomes steeper downwards. Thus, the value of the function is becoming increasingly negative at an increasing rate.

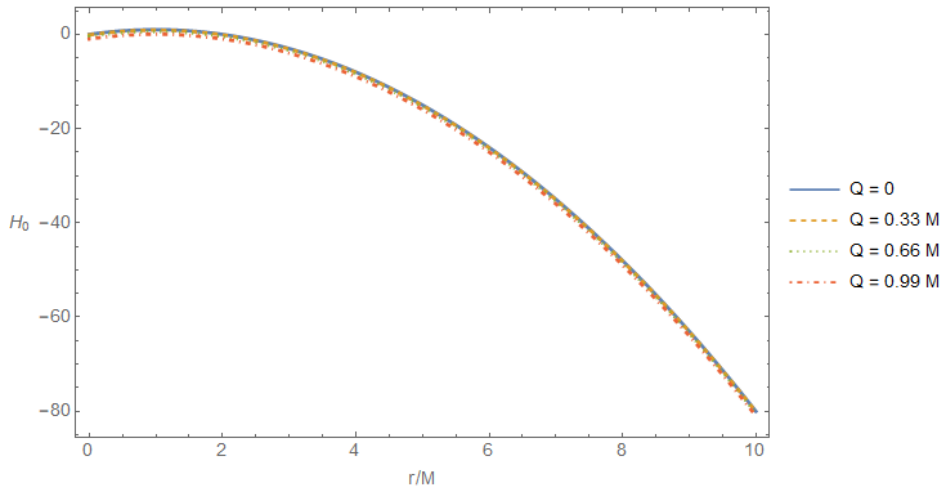

Figure 3.1: The C_1 part of the solution $H_0(r/M)$ for different values of Q.

The same holds for the part of the perturbation given by eq. (3.2.11b) that is plotted in figure 3.2: on the scale of the figure, the plot does not change visibly when the charge of the black hole changes. Furthermore, the overall behaviour is similar: upon moving away from the black hole, the absolute value of the perturbation increases at an increasing rate.

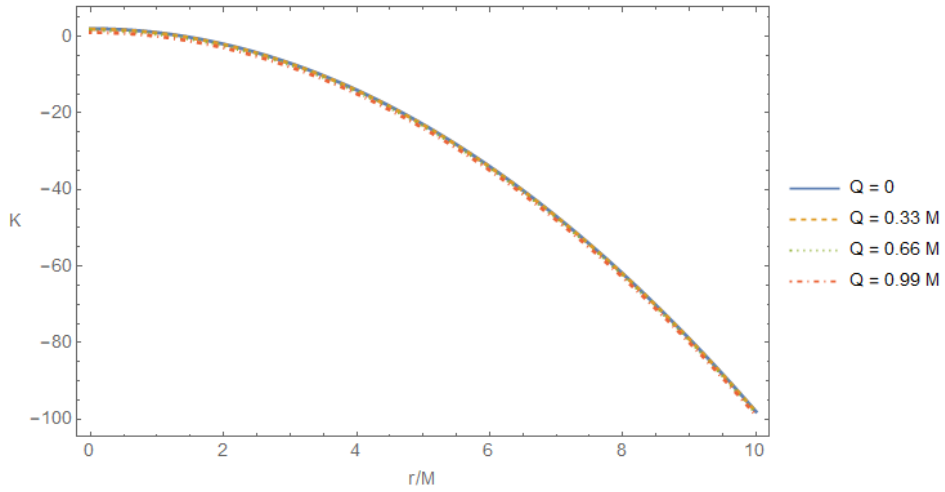

Figure 3.2: The C_1 part of the solution $K(r/M)$ for different values of Q.

3.3 Schwarzschild black hole in Regge-Wheeler gauge

The expressions for $H_0(r)$ and $K(r)$ for a Schwarzschild black hole (for which $u_i(r) = 0$) in the Regge-Wheeler gauge can be found by solving the vacuum Einstein equations. These are simply $G_{\mu\nu} = 0$ since there is no stress-energy tensor in this case. An even more efficient way of obtaining these solutions is by taking the limit $Q \to 0$ in the solutions of the Reissner-Nordström black hole. Since these solutions have already been found, the latter method is more efficient. Both methods should yield the same result thereby providing a useful check on the calculations.

3.3.1 The limit of the Reissner-Nordström solutions

First consider the part of the solutions given by equations (3.2.10a) and (3.2.10b) proportional to C_{1a} and C_{1b}. When taking the limit $Q \to 0$ of the terms, the resulting expressions do not solve the vacuum Einstein equations. An additional condition must be obeyed before all Einstein equations return zero. It is logical that this additional condition is required, since the nonvacuum solutions contain three free constants C_{1a}, C_{1b} and C_2 whereas the vacuum solutions only have two degrees of freedom (two independent solutions). The condition is: $C_{1a} = -4C_{1b}$, which indeed leaves two free constants in the vacuum solutions. This condition was derived by plugging the $Q \to 0$ limit of the expressions for $H_0(r)$ and $K(r)$ into the vacuum Einstein equations. Not all components of these returned zero unless the condition $C_{1a} = -4C_{1b}$ was obeyed.

There was a seemingly similar problem with the term proportional to C_2 since the limit $Q \to 0$ of that term did not solve the vacuum Einstein equations. However, in this case there is not the possibility to combine two constants since there is only one. Initially, this part of the solution was given as a complex function containing an arctan, which was rewritten with the hope that it would solve the problem. Unfortunately, in the form it has in eq. (3.2.10) the problem persists. Based on the solutions for the Reissner-Nordström black hole, the expectation was that there would be another solution in the Schwarzschild case as well. Therefore, the vacuum Einstein equations were solved nonetheless, to see if that yielded any additional solutions. Apart from the same solution as was obtain by taking the limit $Q \to 0$ of the Reissner-Nordström solutions, another solution was indeed also found.

By combining the results from both methods, the following expressions for $H_0(r)$ and $K(r)$ for a

Schwarzschild black hole are then obtained:

$$H_0(r) = \frac{1}{(2M-r)r}\left[C_2\left((12M^2r^2 - 12Mr^3 + 3r^4)\log\left[1-\frac{2M}{r}\right] + 4M^4 + 8M^3r - 18M^2r^2 + 6Mr^3\right)\right.$$
$$\left. + C_1(4M^2r^2 - 4Mr^3 + r^4)\right] \tag{3.3.1a}$$
$$H_1(r) = 0 \tag{3.3.1b}$$
$$H_2(r) = H_0(r) \tag{3.3.1c}$$
$$K(r) = \frac{1}{r}\left[C_2\left((6M^2r - 3r^3)\log\left[1-\frac{2M}{r}\right] + 4M^3 - 6M^2r - 6Mr^2)\right) + C_1(2M^2r - r^3)\right]. \tag{3.3.1d}$$

So, the solution proportional to C_1 was found with both methods whereas the solution porportional to C_2 was only found by solving the vacuum Einstein equations. Therefore, the constant C_2 is (most likely) not the same as the one that is in the expressions of equation (3.2.10).

Equation (3.3.1) contains the expressions encoding the radial dependence of the perturbation of the Schwarzschild metric in the Regge-Wheeler gauge. The expressions contain two dimensionless constants, meaning that they represent a combination of two independent solutions. Unfortunately, the part of the solutions of the Reissner-Nordström perturbation proportional to C_2 do not carry over to the Schwarzschild solution proportional to C_2 in the limit $Q \to 0$. This discrepancy will be elaborated on later.

The full set of equations that the above expression solve can be derived from equations found in the Appendix. This is done by taking the limit $Q \to 0$ of the Einstein equations of the Reissner-Nordström black hole in the Regge-Wheeler gauge. The functions $u_1(r)$, $u_2(r)$ and $u_3(r)$ all become zero, as they should since we are now dealing with a neutral black hole which is described by the vacuum Einstein equations.

3.3.2 Behaviour of the Schwarzschild perturbation in the Regge-Wheeler gauge

This section contains plots of both (parts) of the solutions for the functions $H_0(r)$ and $K(r)$ as a function of the dimensionless r/M. In these plots, the part corresponding to $H_0(r)$ is represented by a solid red line and the part corresponding to $K(r)$ is represented by a dotted blue line. The first plot depicts the C_1 part of either of the solutions and the second plot shows the C_2 part.

The lines in figure 3.3 can also be found by taking the line corresponding to $Q = 0$ in figures 3.2.11a and 3.2.11b. In other words, the plot shown in figure 3.3 is already contained in the previous ones, thus they will only be described briefly here. The plot starts at the center of the black hole at $r = 0$. Due to the fact that the solutions are described in terms of Eddington-Finkelstein coordinates, the solutions are also valid inside the event horizon at $r/M = 2$. The lines corresponding to this first part of the solutions are decreasing. However, since they start around zero the fact that they go down means that they become increasingly negative.

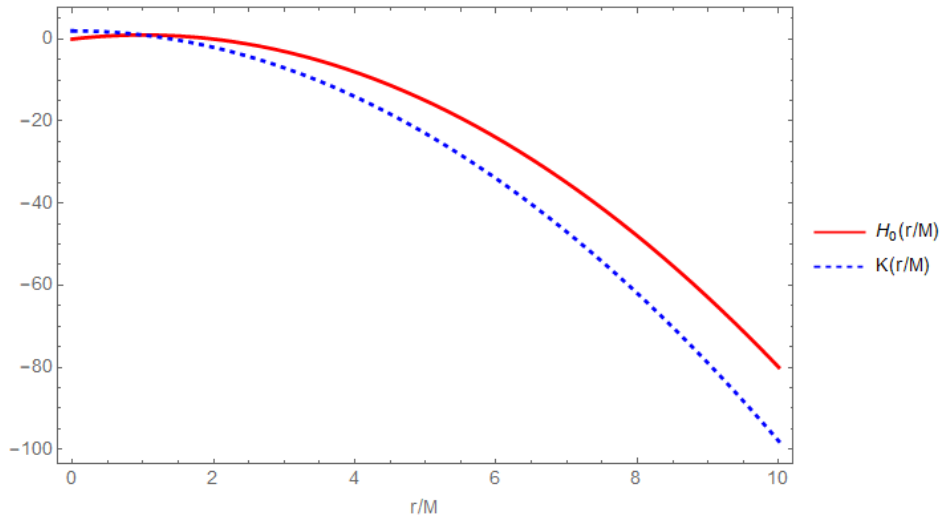

Figure 3.3: The C_1 part of the expressions $H_0(r/M)$ (in solid red) and for $K(r)$ (in dashed blue) as a function of the dimensionless r/M.

The lines plotted in figure 3.4 do not have a corresponding one in the plots of the Reissner-Nordström perturbation. In this figure, the horizontal axis starts from a value of 2 for r/M which represent the position of the horizon of the black hole. At the horizon of the black hole both terms are infinitely large, which can also be concluded from plugging $r = 2M$ into the corresponding expression. Upon moving away from the horizon, both lines decrease, similar to the plot of the first solution. However, in this case the lines are moving towards zero, meaning their absolute value is decreasing, rapidly approaching zero. This means that somewhat away from the black hole, these terms can already be neglected. This might be (part of) the reason why finding a solution for the Reissner-Nordström perturbation that resulted in term plotted here in the limit $Q \to 0$ was unsuccessful (again, more in this later).

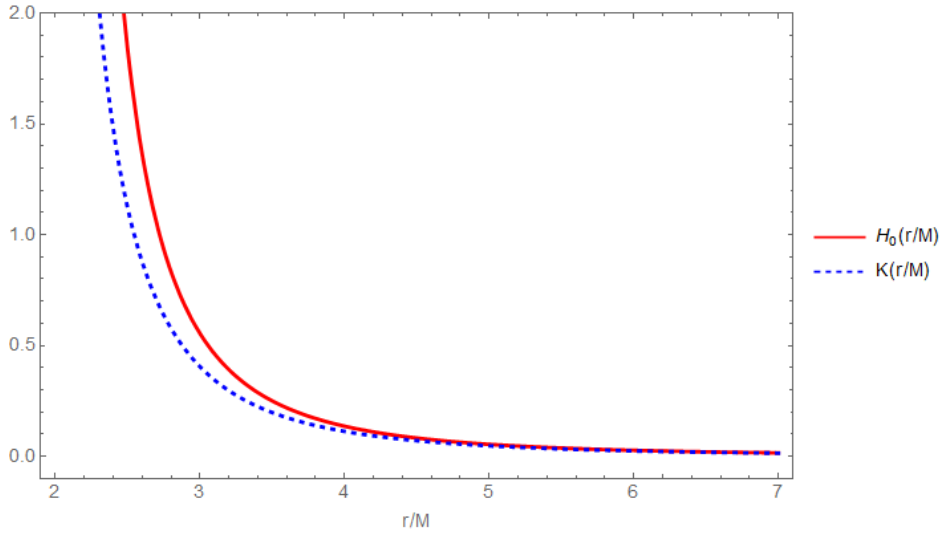

Figure 3.4: The C_2 part of the expressions $H_0(r/M)$ (in solid red) and for $K(r)$ (in dashed blue) as a function of the dimensionless r/M.

From the above it can be concluded that the first part of the solutions of $H_0(r)$ as well as $K(r)$ quickly

becomes dominant over the second part upon moving away from the singularity.

3.4 Reissner-Nordström black hole in light cone gauge

In this section, the procedure described above will be repeated in the light cone gauge. Since a different gauge simply represents a different way of describing the same black hole, the equations involved are still Einstein's and Maxwell's equations. The equations will look differently and contain different undetermined functions of r as the perturbation is restricted by different gauge conditions.

3.4.1 Metric perturbation

With the restrictions on the metric perturbation given by the light cone gauge conditions, the non-zero components of the perturbed metric in the light cone gauge can be written as follows:

$$g_{vv} = -f - r^2 e_1 \mathcal{E}^q \varepsilon + O[\varepsilon]^2 \tag{3.4.1a}$$
$$g_{vr} = 1 \tag{3.4.1b}$$
$$g_{vA} = -\frac{2}{3} r^3 e_4 \mathcal{E}^q_A \varepsilon + O[\varepsilon]^2 \tag{3.4.1c}$$
$$g_{AB} = r^2 \Omega_{AB} - \frac{1}{4} e_7 \mathcal{E}^q_{AB} \varepsilon + O[\varepsilon]^2. \tag{3.4.1d}$$

The $e_1(r)$, $e_4(r)$ and $e_7(r)$ are the functions of r describing the perturbation in the light cone gauge and that are to be determined by means of Einstein's equations.

3.4.2 The perturbation functions

The procedure to determine the right-hand side of Einstein's equations is the same as in the Regge-Wheeler gauge and again involves the functions $u_1(r)$, $u_2(r)$ and $u_3(r)$. However, it cannot a priori be assumed that these are the same functions as the ones in the Regge-Wheeler gauge. Therefore, they will have to be determined again, which can proceed in a similar way as for the Regge-Wheeler gauge by plugging them into Einstein's equations. However, these equations turned out to be too difficult to solve directly. Even trying similar things as before, like combining two equations or writing one parameter in terms of the others proved unsuccessful. Therefore, a different coordinate system was eventually chosen with t instead of v, in which the background metric is diagonal and the electromagnetic potential is also less complicated.

In this coordinate system, the Einstein and Maxwell equations where solved, with the following results:

$$\begin{aligned} e_1(r) = \frac{1}{3r^5}\Bigg[& C_{1a}\Big(-2Mr(-3MQ^2 + 4M^2 r + 2Q^2 r - 4Mr^2 + r^3)\Big) \\ & + C_{1b}\Big(r(16M^3 r + 3(Q^2 + r^2) - 4Mr(Q^2 + 2r^2))\Big) + C_3\big(6M^3(-Q^2 + Mr)\big)\Bigg] \end{aligned} \tag{3.4.2}$$
$$e_4(r) = \frac{1}{r^5}\left[C_{1a}\Big(M(2M - r)r^3\Big) + C_{1b}\Big(r^3(-4M^2 + Q^2 + r^2)\Big) + C_3\big(M^3 f r^2\big)\right] \tag{3.4.3}$$
$$e_7(r) = \frac{1}{3r^3}\left[C_{1a}\Big(2M(4M - 3r)r\Big) + C_{1b}\Big(r(-22M^2 + 12Mr + 3(Q^2 + r^2))\Big) - C_3\big(6M^3\big)\right] \tag{3.4.4}$$
$$\begin{aligned} u_1(r) = \frac{1}{6Qr}\Bigg[& C_{1a}\Big(2Mr(2M^2 r + 2Q^2 r + r^3 - 3M(Q^2 + r^2))\Big) \\ & + C_{1b}\Big(-r(8M^3 r + (3Q^2 - 12M^2)(Q^2 + r^2) + 2Mr(Q^2 + 2r^2))\Big) + C_3\big(6M^3 Q^2\big)\Bigg] \end{aligned} \tag{3.4.5}$$

In the Regge-Wheeler gauge, a term was found that did not have the right limit $Q \to 0$, but such a term was not found in the light cone gauge. However, there was an additional term without any log or arctan. Hence, the expressions now contain three undetermined, dimensionless constants without a log term, which

is one more than in the Regge-Wheeler gauge. There is an additional C_3 term that is not present in the Regge-Wheeler gauge, which is why the constant was called C_3. A gauge transformation must exist between the Regge-Wheeler and light cone gauge. However, such a transformation would only make sense if the solutions in both gauge have the same number of degrees of freedom. Therefore, there most be some way to get rid of this additional constant in the light cone gauge. As it turns out there is and it is due to the fact that there is residual gauge freedom in the light cone gauge.

In a later section, it will be explained how it was attempted to find a solution containing a log, similar to the term proportional to C_2 in the Regge-Wheeler gauge.

3.4.3 Exploiting residual gauge freedom

The $e_1(r)$, $e_4(r)$ and $e_7(r)$ are expressions representing the perturbation of the Reissner-Nordström black hole in the light cone gauge. The three constants C_{1a}, C_{1b} and C_3 are as of yet undetermined constants, independent of r. As was noted, compared to the perturbation in the Regge-Wheeler gauge, there is an additional constant in this case. This is undesirable since a gauge transformation must exist between the solutions in both gauges, which is not possible if they have a different number of degrees of freedom.

It is possible that this additional constant is a manifestation of the residual gauge freedom present in the light cone gauge, which will be investigated now. First recall from eq. (2.4.7) how the residual gauge freedom affects the perturbation functions and use: $h_{vv} = -r^2 e_1(r)\mathcal{E}^q(\theta,\phi)$. Only looking at r dependent term proportional to C_2 and plug it into a version of eq. (2.4.7a) that includes the charge:

$$h_{vv}(r) = ... + \frac{M^3(Mr-Q^2)}{r^3}C_2. \tag{3.4.6}$$

Since this term must be cancelled, we must have:

$$h'_{vv} = ... + \frac{M^3(Mr-Q^2)}{r^3}C_3 + 2\frac{Mr-Q^2}{r^3}b = 0 \tag{3.4.7}$$

which is zero if $b = -\frac{1}{2}C_3M^3$.

Then looking at $h_{vA} = j_v Y_A = -\frac{2}{3}r^3 e_4(r)\mathcal{E}^q_A(\theta,\phi)$, which leads to: $j_v(r) = -\frac{1}{3}r^3 e_4(r)$. When this is plugged into equation 2.4.7b, the following term proportional to C_3 is obtained:

$$j'_v = ... + \frac{M^3(2r(M+r)-Q^2}{6r^2}C_3 + af + \frac{1}{2}M^3C_3 \tag{3.4.8}$$

$$= ... + (1 - \frac{2M}{r} + \frac{Q^2}{r^2})a + (1 - \frac{2M}{r} + \frac{Q^2}{r^2})\frac{1}{6}M^3C_3. \tag{3.4.9}$$

This can be made zero by setting $a = -\frac{1}{6}M^3C_3$.

There is still $e_7(r)$, which features in $h_{\theta\theta} = -\frac{1}{3}r^4 e_7(r)\mathcal{E}^q_{\theta\theta}(\theta,\phi)$. Using $\mathcal{E}^q_{AB}(\theta,\phi) = \mathcal{E}^q Y_{AB}(\theta,\phi)$ (where summation over repeated suppressed multipole indices is implied [9]) we can read off: $K = 0$ and $G = -\frac{1}{3}r^4 e_7(r)$. This can be plugged into equation 2.4.7d to obtain:

$$\begin{aligned} G' &= ... - \frac{1}{3r}M^3C_3 - \frac{2}{r}a - 2c \\ &= ... - \frac{1}{3r}M^3C_3 + \frac{2M^3}{6r}C_3 - 2c \end{aligned}$$

Since the first two terms already cancel, we can set $c = 0$. From this it can be concluded that the C_3-term in the light cone gauge solutions can be considered a manifestation of the residual gauge freedom in this gauge [3]. This means that one of the solutions can be cancelled by setting $a = -\frac{1}{6}M^3C_3$, $b = -\frac{1}{2}C_3M^3$ and $c = 0$ in the functions generating the residual gauge freedom. Thus there is a freedom to remove the C_3 solution while remaining in the light cone gauge, which is why that solutions will be disregarded from now on.

3.4.4 Behaviour of Reissner-Nordström perturbation in the light cone gauge

This section contains plots of the three functions describing the metric perturbation, as a function of the dimensionless variable r/M. Each plot contains multiple lines, with each line corresponding to a different value of Q, from 0 to very close to M. The scale of the horizontal axis is the same as it was in the plots for the Regge-Wheeler gauge.

For the same reason as in the Regge-Wheeler gauge, that the solutions for the Reissner-Nordström perturbation must solve the vacuum Einstein equations in the limit $Q \to 0$, the condition $C_{1a} = 2C_{1b} = C_1$ must now hold. This means that the plots below are of the following functions:

$$e_1(r) = \frac{r(Q^2 + r(-2M + r))^2}{r^5} C_1 \tag{3.4.10a}$$

$$e_4(r) = \frac{Q^2 + r(-2M + r)}{r^2} C_1 \tag{3.4.10b}$$

$$e_7(r) = \frac{Q^2 - 2M^2 + r^2}{r^2} C_1 \tag{3.4.10c}$$

Figure 3.5 shows $e_1(r/M)$ for four different values of Q. In this case, the different lines are somewhat different from each other inside or close to the (outer) horizon, which is at most at the radial position $2M$. Since these solutions describe the same physics but in a different gauge, it might seem contradictory that the value of Q does seem to matter in the light cone gauge but not in the Regge-Wheeler gauge. However, the scale of the vertical axis is a factor of 10^2 smaller, which means that any differences are enhanced by that same factor. This means that the effect of a change in Q is not necessarily different, just more visible in this case. Upon moving further away from the horizon the different lines get closer together, until they can hardly be distinguished. With this different scale, the behaviour far away from the black hole still looks the same: the perturbation barely depends on the charge of the black hole.

The overall behaviour of $e_1(r/M)$, regardless of the value of Q, is that it becomes increasingly negative (i.e. its absolute value is increasing) upon moving further away from the black hole. However, recall that the horizontal axis only runs up to a value of 10 for r/M, which is quite a small value on an astronomical scale. If the horizontal axis were to continue up to a much larger value of r/M, the lines would not continue to go down but would asymptotically approach -1. Hence they will not become infinitely large.

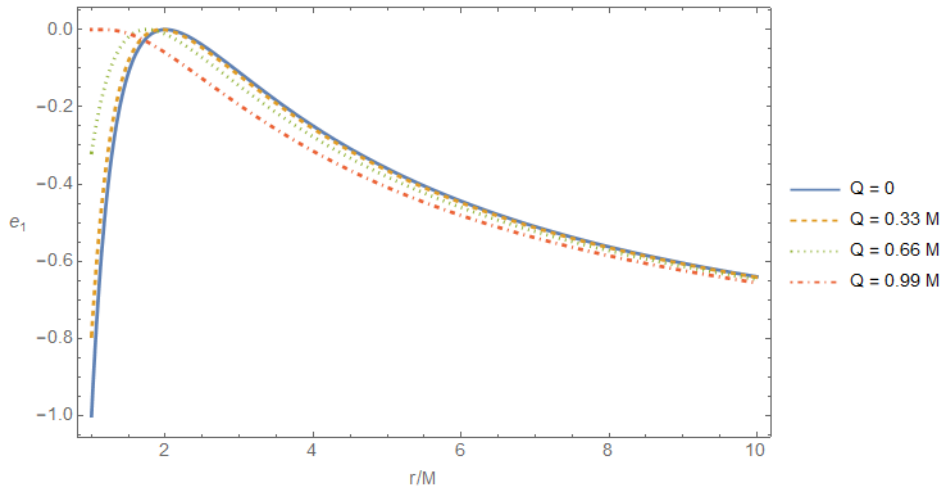

Figure 3.5: The C_1 part of the solution $e_1(r/M)$ for different values of Q.

The function $e_4(r/M)$ is plotted in figure 3.6 for the same four values of Q and shows similar behaviour: Close to or inside the horizon the charge Q seems to have some effect, but with increasing r/M, the lines

corresponding to different Q effectively merge. The overall behaviour is also similar in that the absolute value of $e_4(r/M)$ is increasing upon moving away from the black hole. Again, only a small part of space is plotted to zoom in on the differences near the horizon. If a much larger part of space had been plotted, it would be visible that $e_4(r/M)$ never moves below -1, meaning that it does not diverge.

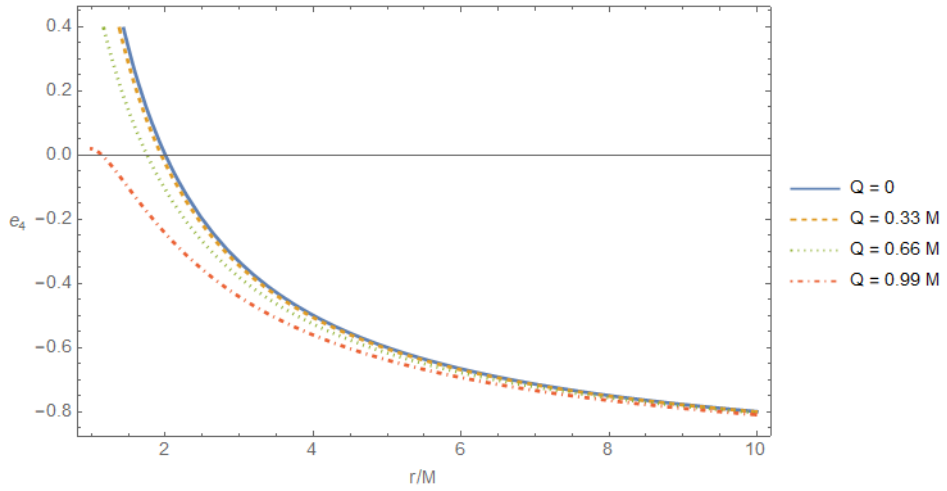

Figure 3.6: The C_1 part of the solution $e_4(r/M)$ for different values of Q.

The third part of the C_1 solution of the perturbation also behaves similarly: The value of Q only slightly matters near or inside the black hole and $e_7(r/M)$ approaches -1 as r/M increases.

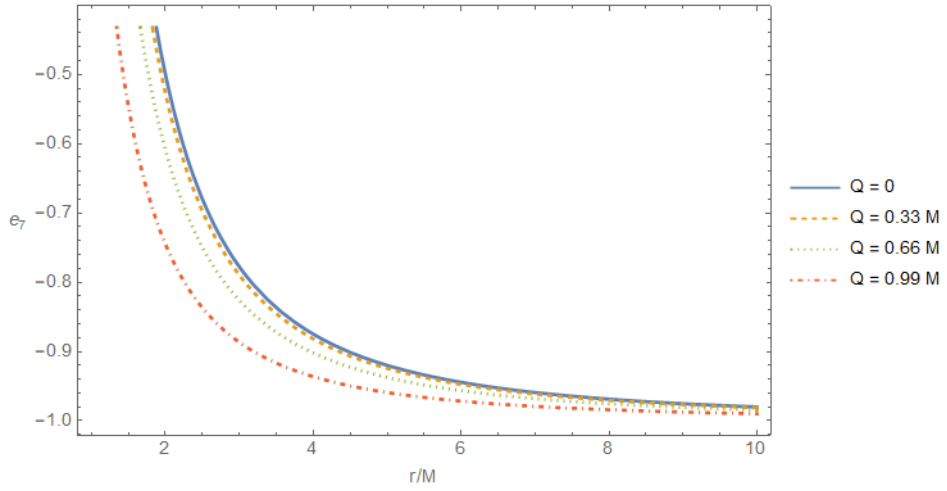

Figure 3.7: The C_1 part of the solution $e_7(r/M)$ for different values of Q.

That the absolute value of the dominant part of the solutions continues to increase in the Regge-Wheeler gauge whereas it quickly approaches a constant value in the light cone gauge might seem problematic. However, it is important to note that the Regge-Wheeler gauge expressions $H_0(r)$ and $K(r)$ appear in the perturbation as they are, whereas the light cone gauge expressions $e_1(r)$, $e_4(r)$ and $e_7(r)$ have an additional factor of r^2, r^3 and r^3 in front respectively. Taking these factors into account, the expressions corresponding to the Regge-Wheeler gauge and the light cone gauge behave similarly.

3.5 Schwarzschild black hole in light cone gauge

3.5.1 General solution

The Schwarzschild solutions in the light cone gauge can also be found either by solving the vacuum Einstein equations or by taking the limit $Q \to 0$ of the Reissner-Nordström solutions. The full set of solutions that has been found by a combination of these two methods is:

$$e_1(r) = -\frac{1}{r^4}\Bigg[C_1(4M^2r^2 - 4Mr^3 + r^4) \tag{3.5.1a}$$
$$+ C_2\left((12M^2r^2 - 12Mr^3 + 3r^4)\log\left[1 - \frac{2M}{r}\right] + 4M^4 + 8M^3r - 18M^2r^2 + 6Mr^3\right) + C_3M^4\Bigg]$$
$$e_4(r) = \frac{1}{r^4}\Bigg[C_1(2Mr^3 - r^4) + C_2\left((6Mr^3 - 3r^4)\log\left[1 - \frac{2M}{r}\right] + 4M^4 + 4M^3r + 6M^2r^2 - 6Mr^3\right) \tag{3.5.1b}$$
$$+ C_3(M + r)M^3\Bigg]$$
$$e_7(r) = \frac{1}{r^3}\left[C_1(2M^2r - r^3) + C_2\left((6M^2r - 3r^3)\log\left[1 - \frac{2M}{r}\right] + 4M^3 - 6M^2r - 6Mr^2\right) + C_3M^3\right]. \tag{3.5.1c}$$

Again, the functions $u_1(r)$, $u_2(r)$ and $u_3(r)$ are all zero as they should be, since we are again dealing with an uncharged black hole and perturbation. The set contains three dimensionless constants C_1, C_2 and C_3, meaning it represents a combination of three independent solutions, one more than in the Regge-Wheeler gauge.

The solution proportional to C_1 was found by taking the limit $Q \to 0$ of the Reissner-Nordström solutions and then setting $C_{1a} = 2C_{1b} = C_1$, as required for the solution to also solve the vacuum Einstein equations. The solution proportional to C_3 was found by taking the same limit, and no constraints on that constant were required. The solution proportional to C_2 was found by solving the vacuum Einstein equations in the light cone gauge. The latter method also reproduced the other two solutions, proportional to C_1 and C_3.

3.5.2 Exploiting residual gauge freedom

It will now be checked whether the additional solution proportional to C_3 for the perturbation of a Schwarzschild black hole can also be removed without moving out of the light cone gauge. This will be done by using the same expressions as for the Reissner-Nordström solutions, only without Q, which means eq. 2.4.7 can be used.

The following still holds: $h_{vv}(r) = -r^2e_1(r) = ... + \frac{M^4}{r^2}C_2$. Plugging this into equation 2.4.7a now gives:

$$h'_{vv} = ... + \frac{M^4}{r^2}C_3 + \frac{2M}{r^2}b,$$

which is indeed equal to zero when the b that was found earlier ($b = -\frac{1}{2}C_3M^3$) is plugged in.

Plugging the relevant term into equation 2.4.7b yields:

$$\begin{aligned} j'_v &= ... - \frac{(M + r)}{3r}M^3C_3 + f(r)a + \frac{1}{2}M^3C_3 \\ &= ... + (1 - \frac{2M}{r})a - \frac{M^4}{3r}C_3 + \frac{1}{6}M^3C_3 \\ &= ... + (1 - \frac{2M}{r})a + \frac{1}{6}(1 - \frac{2M}{r})M^3C_3. \end{aligned}$$

This is also zero when plugging in $a = -\frac{1}{6}M^3C_3$ that was found in the case with charge.

The condition $c = 0$ also leads to the right result when plugged into equation 2.4.7d:

$$\begin{aligned} G' &= ... - \frac{1}{3r}M^3C_3 - \frac{2}{r}a - 2c \\ &= ... - \frac{1}{3r}M^3C_3 + \frac{2M^3}{6r}C_3 - 2c, \end{aligned}$$

as the term proportional to C_3 is indeed cancelled. This means that one of the solutions can be cancelled by setting $a = -\frac{1}{6}M^3C_3$, $b = -\frac{1}{2}C_3M^3$ and $c = 0$ in the functions generating the residual gauge freedom. Thus there is a freedom to remove the C_3 solution while remaining in the light cone gauge, which is why that part of the solutions will be disregarded from now on.

3.5.3 Behaviour of the Schwarzschild perturbation in the light cone gauge

Now that the problem of a different number of degrees of freedom has been fixed, the remaining solutions of the Schwarzschild perturbation in the light cone gauge will be plotted. Both (parts) of the solutions will be shown in different plots, all as a function of the dimensionless r/M.

All lines in figure 3.8 become increasingly negative with increasing r/M. However, the slope of each line is decreasing, meaning the absolute value of the functions is increasing but the speed with which this happens is dropping. Eventually, all functions appear to reach a plateau after which they remain approximately constant, that is, they all reach a value of -1 asymptotically.

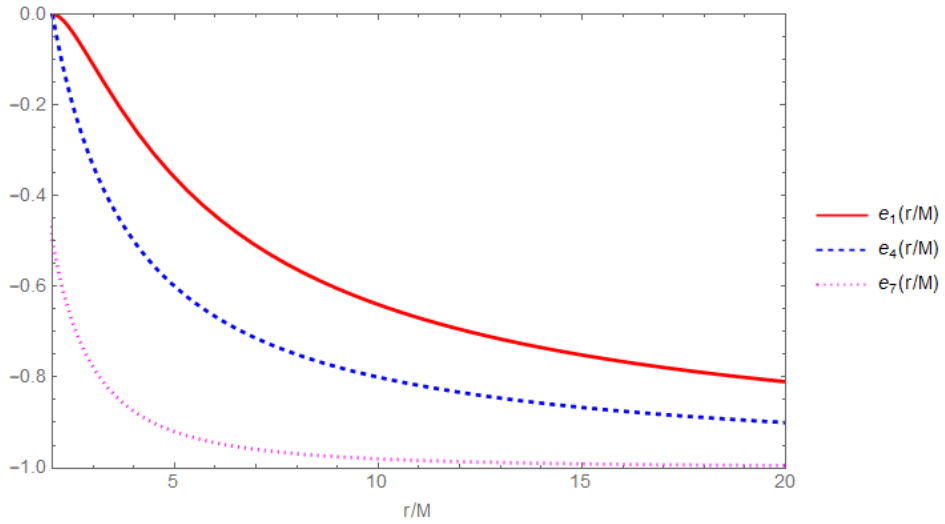

Figure 3.8: The C_1 part of the expressions $e_1(r/M)$ (in solid red), $e_4(r/M)$ (in dashed blue) and $e_7(r/M)$ (in dotted green) as a function of the dimensionless r/M.

Figure 3.9 is a plot of the C_2 solutions containing the $\log\left[1 - \frac{2M}{r}\right]$ term. As was the case in the Regge-Wheeler gauge, the lines representing these solutions quickly approach zero with increasing r/M. Therefore, the C_1 part becomes dominant over the C_2 part, as the latter becomes zero.

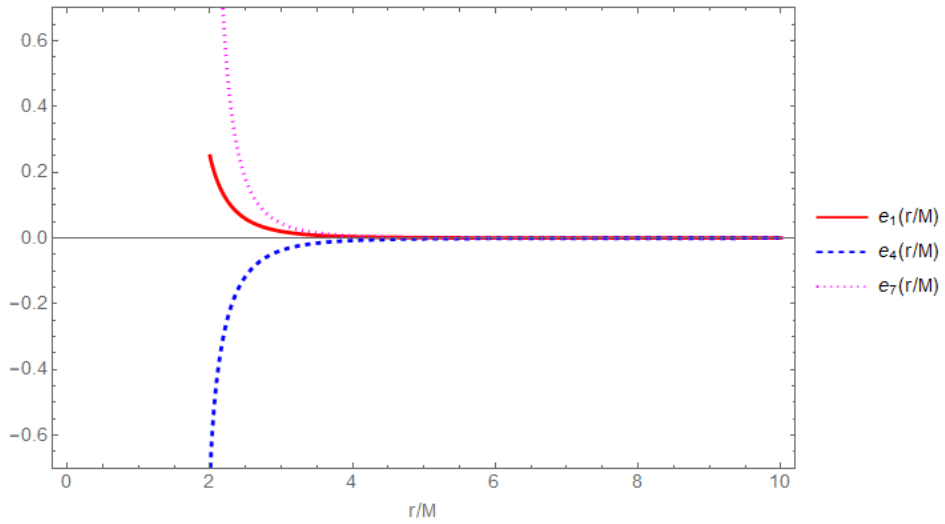

Figure 3.9: The C_2 part of the expressions $e_1(r/M)$ (in solid red), $e_4(r/M)$ (in dashed blue) and $e_7(r/M)$ (in dotted green) as a function of the dimensionless r/M.

3.5.4 Additional constraints

The solutions for a neutral black hole are constrained by physical requirements, the first one being that the functions must be well-behaved at the event horizon ($r = 2M$). This leads to the requirement that $C_2 = 0$ since the logarithm diverges as $r \to 2M$. The second constraint is that the functions must approach unity as $r \to \infty$ by the black hole no-hair theorem. This limit will be investigated for the e_1-function, but for the other functions the procedure is quite similar. In the C_1-term, the r^4 part then becomes dominant, which has a $-1/r^4$ in front, so it becomes $-C_1$. This leads to: $e_1(r \to \infty) \approx -C_1 = 1$, which fixes $C_1 = -1$. With these choices, the results in [9] are recovered.

3.6 Gauge transformations

Now that expressions have been found for the perturbations of a Reissner-Nordström and Schwarzschild black hole in both the Regge-Wheeler and light cone gauge, a gauge transformation can be found between these expressions. This will first be done for the perturbations of the Reissner-Nordström black hole, when the functions that generate the transformation will contain Q. In the following part, it will be checked if these functions in the limit $Q \to 0$ generate a transformation for the Schwarzschild solutions.

3.6.1 Gauge tranformation of Reissner-Nordström perturbation

The goal of this section is to find a tranformation that will convert the expression for the metric perturbation in the Regge-Wheeler gauge to that in the light cone gauge and vice versa. First, the general eq. 2.4.1 will be written out into components, with the transformed perturbation functions p'_{ab} denoting the ones in the light cone gauge and the original p_{ab} denoting those in the Regge-Wheeler gauge. The generators of the gauge transformation in its component form again involves a multipole expansion: $\xi_\mu(r,\theta,\phi) = (\xi_v(r)\mathcal{E}^q(\theta,\phi), \xi_r(r)\mathcal{E}^q(\theta,\phi), \xi(r)\nabla_\theta\mathcal{E}^q(\theta,\phi), \xi(r)\nabla_\phi\mathcal{E}^q(\theta,\phi))$. This means expressions are to be found for the functions $\xi_v(r)$, $\xi_r(r)$ and $\xi(r)$ to completely describe the gauge transformation.

The vv-component of these equations is: $h'_{vv}(r) = -r^2 e_1(r) - 2\nabla_v\xi_v$. The covariant derivative can be written out: $\nabla_v\xi_v = \partial_v\xi_v - \Gamma^\lambda_{vv}\xi_\lambda$, where the Christoffel symbols Γ^λ_{vv} can be calculated from the unperturbed metric since only perturbations up to first order are considered. Because time-dependence is neglected, $\partial_v\xi_v = 0$. The only non-zero Christoffel symbols with lower indices vv are: $\Gamma^v_{vv} = \frac{-Q^2+Mr}{r^3}$ and

$\Gamma^r_{vv} = \frac{-Q^2+Mr}{r^3} f$.

Performing similar steps for the other components yields the following set of six equations for $\xi_v(r)$, $\xi_r(r)$, $\xi(r)$:

$$r^2 e_1(r) + f H_0(r) + 2\frac{-Q^2+Mr}{r^3}\xi_v(r) + 2\frac{-Q^2+Mr}{r^3} f\xi_r(r) = 0 \tag{3.6.1a}$$

$$\partial_r \xi_r(r) - \frac{H_0(r)}{f} = 0 \tag{3.6.1b}$$

$$\partial_r \xi_v(r) - 2\frac{-Q^2+Mr}{r^3}\xi_r(r) + H_0(r) = 0 \tag{3.6.1c}$$

$$\frac{1}{3} r^3 e_4(r) - \xi_v(r) = 0 \tag{3.6.1d}$$

$$\left(\frac{2}{r} + \partial_r\right)\xi(r) - 2\xi_r(r) = 0. \tag{3.6.1e}$$

Since three functions $\xi_v(r)$, $\xi_r(r)$, $\xi(r)$ have to be found to specify the radial part of the gauge transformation, only three equations are required. Therefore, two of the equations above are redundant.

Equations (3.6.1b), (3.6.1d) and (3.6.1e) were used to find solutions for $\xi_v(r)$, $\xi_r(r)$ and $\xi(r)$:

$$\xi_v(r) = \left(-r + \frac{r^2}{2M}\right) C_{1a} + \left(-4r + \frac{4r^2}{3M} + \frac{(Q^2+r^2)r}{3M^2}\right) C_{1b} \tag{3.6.2a}$$

$$\xi_r(v) = -\frac{r^2}{2M} C_{1a} - \left(\frac{r^3}{3M^2} + \frac{2r^2}{M}\right) C_{1b} \tag{3.6.2b}$$

$$\xi(r) = -\frac{r^3}{5M} C_{1a} - \left(\frac{4r^3}{5M} + \frac{r^4}{9M^2}\right) C_{1b}. \tag{3.6.2c}$$

The constants C_{1a} and C_{1b} are the same as the ones that appear in the metric perturbation in both gauges. Hence they are still dimensionless, even though it may not appear to be the case based on the above expressions. There is no part of the expression that is proportional to C_2, as no solution proportional to this constant was found in the light cone gauge.

Since it would be desirable to have the same amount of solutions in either gauge due to gauge invariance, an alternative method to find the third solution in the light cone gauge was tried. It involved finding expressions for the functions $\xi_v(r)$, $\xi_r(r)$ and $\xi(r)$ generating the gauge transformation proportional to C_2 from only knowing the solution in the Regge-Wheeler gauge. In principle, not knowing the solutions in the light cone gauge - since that is the one to be determined - was not a problem, as it only involves picking the right components of the general gauge transformation equation. Equations (3.6.1b), (3.6.1c) and (3.6.1e) only contain the functions generating the gauge transformation and the perturbation functions of the Regge-Wheeler gauge. Thus, these equations could be solved for the generators $\xi_v(r)$, $\xi_r(r)$ and $\xi(r)$ which could then be plugged into the other gauge transformation equations to find solutions for $e_1(r)$, $e_4(r)$ and $e_7(r)$. However, plugging the Regge-Wheeler solutions into the aforementioned equations lead to differential equations that could not be solved directly.

3.6.2 Gauge transformation of Schwarzschild perturbation

To find the functions generating the gauge transformation of the Schwarzschild solution from the Regge-Wheeler to the light cone gauge, the same procedure can be used. First, equation 2.4.1 is written out into components to obtain multiple equations. The components of the metric perturbation featuring the functions $H_0(r)$, $K(r)$, $e_1(r)$, $e_4(r)$ and $e_7(r)$ can be plugged into these equations. The Christoffel symbols must also be calculated, in this case from the background Schwarzschild metric. The relevant equations can also be obtained by taking the limit $Q \to 0$ of the Reissner-Nordström transformation equations. These can then

be solved to find the generators of the gauge transformation of the Schwarzschild solutions. An even more direct method is to take the limit $Q \to 0$ of the solution in eq. (3.6.2) and remember that this limit entails the condition $C_{1a} = 4C_{1b} = C_1$ in the Regge-Wheeler gauge.

Using the latter method leads to the following expressions for $\xi_v(r)$, $\xi_r(r)$ and $\xi(r)$:

$$\xi_v(r) = \frac{r^2(-2M+r)}{3M^2} C_1 \tag{3.6.3a}$$

$$\xi_r(r) = -\frac{r^3}{3M^2} C_1 \tag{3.6.3b}$$

$$\xi(r) = -\frac{r^4}{9M^2} C_1. \tag{3.6.3c}$$

When these are plugged into the gauge transformation equations it turns out that they indeed transform perturbation in the Regge-Wheeler gauge to that in the light cone gauge.

3.6.3 Alternative, trial solution

In the limit $Q \to 0$, the solution for the Reissner-Nordström black hole in the Regge-Wheeler gauge proportional to C_2 does not lead to the Schwarzschild solution proportional to C_2. And, the expression that this limit does lead to does not solve the vacuum Einstein equations. Due to this inconsistency, an alternative solution was searched for, the form of which was derived from the C_2 part of the solution of the Schwarzschild black hole such that it would lead to that solution in the limit $Q \to 0$. The following trial solution was attempted for the part of $H_0(r)$ and $K(r)$ proportional to C_2:

$$H_0(r) = f_1[r, M, Q] + f_2[r, M, Q] \log\left[1 - \frac{2M}{r} + \frac{Q^2}{r^2}\right] \tag{3.6.4a}$$

$$K(r) = f_3[r, M, Q] + f_4[r, M, Q] \log\left[1 - \frac{2M}{r} + \frac{Q^2}{r^2}\right] \tag{3.6.4b}$$

$$u_1(r) = f_5[r, M, Q] + f_6[r, M, Q] \log\left[1 - \frac{2M}{r} + \frac{Q^2}{r^2}\right] \tag{3.6.4c}$$

with the $f_i[r, M, Q]$ are functions of r, M and Q that are to be determined.

These unknown functions can be determined by plugging them into the Einstein and Maxwell equations. However, now that the functions $H_0(r)$, $K(r)$ and $u_1(r)$ now each contain two new functions, the number of unknowns has doubled. Fortunately, the number of equations also doubled since after the trial solutions are plugged in, each equation can be split up into a part that contains the log and a part that does not. A solution for $f_2[r, M, Q]$, $f_4[r, M, Q]$ and $f_6[r, M, Q]$ was successfully found by setting the combination of factors in front of the log equal to zero in each component of the Einstein and Maxwell equations.

Then expressions for $f_1[r, M, Q]$, $f_3[r, M, Q]$ and $f_5[r, M, Q]$ still had to be found. When looking only at the factors not proportional to the log, it turned out that did not yield equations containing only these functions. The functions $f_2[r, M, Q]$, $f_4[r, M, Q]$ and $f_6[r, M, Q]$ also appeared in these equations due to the fact that the functions were plugged into differential equations containing derivative. And when a derivative is applied to a log, it is not a log anymore. In other words, to find solutions for $f_1[r, M, Q]$, $f_3[r, M, Q]$ and $f_5[r, M, Q]$, equations that contained all six functions $f_i[r, M, Q]$ had to be solved. These equations could not be solved for $f_1[r, M, Q]$, $f_3[r, M, Q]$ and $f_5[r, M, Q]$, even though the other functions were known. Hence, the full expressions for the trial solutions were not found and the method was unsuccessful. Something similar was tried in the light cone gauge with trial solutions for $e_1(r)$, $e_4(r)$, $e_7(r)$ and $u_1(r)$, which unfortunately lead to the same problem.

Chapter 4

Calculating Love numbers

Now that all expressions for the perturbations of the different black holes have been found, the Love numbers of the black holes can be calculated. For the Schwarzschild and Reissner-Nordström black hole, the surficial and gravitational Love numbers will be calculated. In addition, the electromagnetic surficial and far-field Love numbers will be calculated for the Reissner-Nordström black hole. Each subsection will feature the calculation of one of these Love numbers.

4.1 Schwarzschild black hole Love numbers

In this section, the Love numbers of a Schwarzschild black hole are calculated from the metric perturbation. The first paragraph describes the calculation of the surficial Love numbers and the second one that of the gravitational Love numbers.

4.1.1 Surficial Love numbers

It will first be shown that the perturbation function $e_7(r)$ determined in the previous section from Einstein's equations will appear in the expression of the surficial Love numbers [2]. To determine the surficial Love numbers, the deformation caused by the perturbation will be described in terms of a change of the intrinsic curvature of the surface. The intrinsic curvature is described by the Ricci scalar of the corresponding surface. Hence, the Ricci scalar corresponding to the two-dimensional, angular part of the full metric is to be calculated. The result is:

$$\mathcal{R} = \frac{2}{R^2} - 4e_7(r)\mathcal{E}^q(\theta,\phi)\varepsilon + O[\varepsilon^2]. \tag{4.1.1}$$

where R is again the radial position of the horizon. Comparing the expression above with eq. (2.5.1) leads to $\delta\mathcal{R} = -4r^2 e_7(r)\mathcal{E}^q(\theta,\phi)$. The solution that has been found for $e_7(r)$ can then be plugged into this expression, but only if $C_2 = 0$ since that part of the solution diverges at the surface. The expression this results in can be compared to the quadrupole component of eq. (2.5.2):

$$\delta\mathcal{R} = -4h_2\frac{R^3}{M}\mathcal{E}^q(\theta,\phi). \tag{4.1.2}$$

The quadrupolar surficial Love number of a Schwarzschild black hole can be concluded to be:

$$h_2 = \frac{1}{16}(-4C_1). \tag{4.1.3}$$

Using in addition that $C_1 = -1$ leads to $h_2 = 1/4$. This result is in agreement with the general expression from [2]:

$$h_l = \frac{l+1}{2(l-1)}\frac{l!^2}{(2l)!}, \tag{4.1.4}$$

as can be seen by plugging in $l = 2$.

This same procedure can be repeated in the Regge-Wheeler gauge, in which case: $\delta\mathcal{R} = 4K(r)\mathcal{E}^q(\theta,\phi)$. When the expression that has been found for $K(r)$ is plugged in this leads to the same surficial Love number: $h_2 = -\frac{C_1}{4}$ which yields the same value when $C_1 = -1$.

4.1.2 Gravitational Love numbers

Based on section 2.5.2, the gravitational potential up to first order can be written as:

$$U = \frac{M}{r} + \frac{1}{4}r^2 e_1(r)\mathcal{E}^q(\theta,\phi)\varepsilon + O[\varepsilon^2]. \tag{4.1.5}$$

Recalling that the first term M/r is the Newtonian potential of an unperturbed Schwarzschild black hole of mass M, the second term must represent the perturbation of the gravitational potential.

The above expression can be compared to eq. 2.5.7 to obtain:

$$-\frac{1}{2}r^2 e_1(r) = -\sum_{l=2}^{\infty}\frac{1}{(l-1)l}\left[1 + 2k_l(R/r)^{2l+1}\right]r^l \tag{4.1.6}$$

where k_l are the gravitational Love numbers.

The full expression for $e_1(r)$ in powers of $1/r$ is:

$$\begin{aligned} e_1(r) = &-C_1 + (2C_1 + 3C_2)\frac{2M}{r} - (C_1 + \frac{9}{2}C_2)\left(\frac{2M}{r}\right)^2 + C_2\left(\frac{2M}{r}\right)^3 + \frac{1}{4}\left(C_2 - \frac{1}{4}C_3\right)\left(\frac{2M}{r}\right)^4 \\ &+ \left[3C_2 - 6C_2\frac{2M}{r} + 3C_2\left(\frac{2M}{r}\right)^2\right]\ln\left[1 - \frac{2M}{r}\right] + O\left[\frac{M}{r}\right]^6. \end{aligned} \tag{4.1.7}$$

Expanding the $\ln[1 - \frac{2M}{r}]$ in factors of $\frac{1}{r}$ as well yields:

$$\begin{aligned} e_1(r) = ... + &\left[3C_2 - 6C_2\frac{2M}{r} + 3C_2\left(\frac{2M}{r}\right)^2\right] \\ &\cdot\left[-\frac{2M}{r} - \frac{1}{2}\left(\frac{2M}{r}\right)^2 - \frac{1}{3}\left(\frac{2M}{r}\right)^3 - \frac{1}{4}\left(\frac{2M}{r}\right)^4 - \frac{1}{5}\left(\frac{2M}{r}\right)^5 + O\left[\frac{2M}{r}\right]^6\right] \end{aligned} \tag{4.1.8}$$

Writing out the brackets leads to the following $\left(\frac{2M}{r}\right)^5$-term:

$$e_1(r) = ... + \left[-\frac{3}{5} - \frac{6}{4} - \frac{3}{3}\right]C_2\left(\frac{2M}{r}\right)^5 + O\left[\frac{M}{r}\right]^6 = ... + \frac{31}{10}C_2\left(\frac{2M}{r}\right)^5 + O\left[\frac{M}{r}\right]^6, \tag{4.1.9}$$

from which it can be concluded that the quadrupole gravitational Love number for this black hole is: $k_2 = \frac{31}{20}C_2$. Furthermore, by plugging equation (4.1.7) into equation (4.1.6) and paying attention to the factor of $-\frac{1}{2}$ in front it can be derived that $C_1 = -1$, which is in agreement with the result that has been derived before.

However, it was argued that C_2 must be set to zero for $e_1(r)$ to be well-defined everywhere except maybe at $r = 0$. This in turn means that the gravitational Love number for a neutral black hole must be zero. This is in agreement with the conclusion in [5].

The fact that the quadrupole gravitational Love numbers of a Schwarzschild black hole are zero means that the quadrupolar structure of such a black hole at infinity is unaffected by a tidal perturbation [10].

4.2 Reissner-Nordström black hole Love numbers

In this section, the Love numbers for a Reissner-Nordström black hole are calculated.

4.2.1 Surficial Love numbers

As for the Schwarzschild black hole, the surficial Love numbers will be calculated first. The calculation is actually the same, meaning $\delta\mathcal{R} = -4r^2 e_7(r)$. Plugging in the expression for $e_7(r)$ of the Reissner-Nordström black hole and using that the outer horizon at $r = M + \sqrt{M^2 - Q^2}$ is treated as the surface of the black hole yields:

$$h_2 = \frac{2M^2((2M^2 - 3Q^2 + 2M\sqrt{M^2 - Q^2})C_{1a} + (-7M^2 + 9Q^2 - 7M\sqrt{M^2 - Q^2}C_{1b} + 3M^2 C_3))}{3(M + \sqrt{M^2 - Q^2})^4}. \quad (4.2.1)$$

Expanding this expression in powers of Q/M up to second order leads to:

$$h_2 = \frac{2C_{1a} - 7C_{1b}}{12} - \frac{Q^2 C_{1b}}{16M^2} + O\left[\frac{Q}{M}\right]^3 \quad (4.2.2)$$

The conditions $C_{1a} = 2C_{1b} = C_1$ and $C_3 = 0$ that have been derived earlier can then be applied to eq. (4.2.1) to obtain:

$$h_2 = -\frac{2M^2\sqrt{M^2 - Q^2}}{(M + \sqrt{M^2 - Q^2})^3} C_1. \quad (4.2.3)$$

This expression is dimensionless, as any Love number should be by definition.

Figure 4.1 contains a plot of the expression in equation (4.2.3). It shows the quadrupole surficial Love number of the Reissner-Nordström black hole as a function of Q/M, which is between zero and one, since Q can not be larger than M. When Q is equal to zero, $h_2 = 1/4$, which is in agreement with the result that was obtained for the Schwarzschild black hole: $h_2 = -\frac{C_1}{4} = 1/4$. As Q starts to increase with constant M, that is, as Q/M increases, h_2 initially increases above $1/4$. When Q/M gets close to one, that is when Q is almost equal to M, h_2 starts to decrease again, quickly dropping below $1/4$ and decreasing further. Looking at the expression it can be derived that when $Q/M = 1$, i.e. $Q = M$, then $h_2 = 0$.

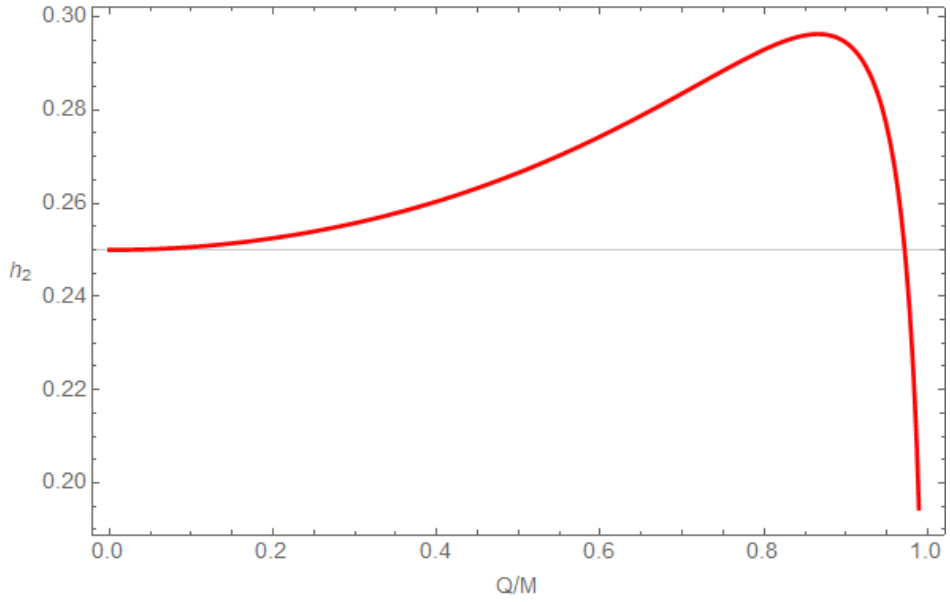

Figure 4.1: The quadrupole surficial Love number of a Reissner-Nordström black hole as a function of Q/M.

4.2.2 Gravitational Love numbers

To calculate the gravitational Love number, the perturbation function $e_1(r)$ must again be expanded in factors of $1/r$. To make the solutions also valid in the limit to an uncharged case, the expression for $e_1(r)$ after applying condition $C_{1a} = 2C_{1b} = C_1$, given in eq. (3.4.10a), will be used. This leads to the following expansion:

$$e_1(r) = C_1 - \frac{2M(C_{1a}+4C_{1b})}{r} + \frac{2(4M^2C_{1a}+(-2M^2+3Q^2)C_{1b})}{r^2} - \frac{4M((2M^2+Q^2)C_{1a}+(-4M^2+Q^2)C_{1b})}{r^3} + \frac{2M^2Q^2C_{1a}+(-M^2Q^2+Q^4)C_{1b}+2M^4C_3}{r^4} - \frac{2M^3Q^2C_3}{r^5} + O\left[\frac{1}{r^6}\right] \tag{4.2.4}$$

To extract the quadrupolar Love number, consider the part of this expansion proportional to $1/r^5$. This only contains the constant C_3, which means the quadrupolar gravitational Love numbers are proportional to C_3. However, it has been shown that the C_3 term of the solution can be gauged away, meaning it can effectively be set to zero. That means that, just as for the Schwarzschild black hole, the quadrupolar gravitational Love numbers of a Reissner-Nordström black hole is zero: $k_2 = 0$. Clearly, it still gives the right result in the limit $Q \to 0$.

4.2.3 Electromagnetic surficial Love numbers

The next two paragraphs describe the calculation of the two kinds of Love numbers that cannot be defined for Schwarzschild black holes. To determine the electromagnetic analogue of the surficial Love numbers, the procedure outlined by Damour & Lecian [8] will be followed. According to eq. 2.5.10 (or [8, equation 58]) the quadrupole electromagnetic surficial Love number is:

$$h_2^{EM} = \frac{4\pi\sigma_2}{\tau_2 R}. \tag{4.2.5}$$

In this expression, σ_2 represent the quadrupole term of the multipole decomposition of the charge density, τ_2 can be extracted from the multipole expansion of the first component of the electromagnetic potential and R is again the radial coordinate of the surface.

To determine the expression for h_2^{EM}, the 0-th component of the electromagnetic potential that contains $u_1(r)$ must be determined, which is:

$$A_0(r,\theta,\phi) = -\frac{Q}{r} + \frac{1}{6Qr^2}\big[2Mr(2M^2r+2Q^2r+r^3-3M(Q^2+r^2))C_{1a} - r(8M^3r+(-12M^2+3Q^2)(Q^2+r^2)+2Mr(Q^2+2r^2))C_{1b}\big]\mathcal{E}^q(\theta,\phi) \tag{4.2.6}$$

This component can be expanded into powers of r, which yields the following expression:

$$A_0(r,\theta,\phi) = ... + \left[\frac{M(C_{1a}-2C_{1b})}{3Q}\right] r^2\mathcal{E}^q(\theta,\phi) + ... \tag{4.2.7}$$

where only the term propotional to r^2 is shown, since that is what τ_2 can be extracted from: $\tau_2 = \frac{M(C_1-2C_2)}{3Q}$.

The multipole expansion of the charge density σ, which can be calculated by taking the r-derivative at the horizon of the 0-th component of the electromagnetic potential, also features in their description. The charge density is:

$$\left[\sigma_2 = \frac{\partial A_0(r)}{\partial r}\right]_{r=M+\sqrt{M^2-Q^2}} = \frac{1}{3Q(M+\sqrt{M^2-Q^2})^3} \cdot \big[(-8M^5+2M^3Q^2+2MQ^4+(-8M^4-2M^2Q^2+3Q^4)\sqrt{M^2-Q^2})C_{1b} + 2M(2M^4-2M^2Q^2+Q^4+(2M^3-MQ^2)\sqrt{M^2-Q^2})C_{1a}\big], \tag{4.2.8}$$

where the subscript 2 indicates that only the quadrupolar part is considered.

Using all this, the quadrupole electromagnetic surficial Love number is found to be:

$$h_2^{EM} = \frac{2(M^4 + (M^3 - MQ^2)\sqrt{M^2-Q^2})C_{1a} + (-4M^4 - 3M^2Q^2 + 3Q^4 + (-4M^3 + MQ^2)\sqrt{M^2-Q^2})C_{1b}}{(M\sqrt{M^2-Q^2})^3(C_{1a} - 2C_{1b})}. \tag{4.2.9}$$

To examine the validity of this expression, a good check is to compare the expression with [8, equation 59]. To be able to compare these expressions it is convenient to expand equation (4.2.9) in factors of Q, leading to:

$$h_2^{EM} = \frac{1}{2} - \frac{3C_{1b}Q^2}{4M^2(C_{1a} - 2C_{1b})} + O\left[\frac{Q}{M}\right]^3 \tag{4.2.10}$$

Next, it is important to remark that in this text we are dealing with a charged black hole in an external field instead of an uncharged black hole in an external field as is the case in [8]. In that case, the Love number for arbitrary l is given by the expression [8, equation 59]:

$$h_l^{EM} = \frac{l!(l+1)!}{(2l)!}$$

When taking the limit $Q \to 0$, the result $(1/2)$ corresponds to the result of setting $l = 2$ in [8, equation 59]. This is an important check on equation (4.2.9) as a valid expression for the electromagnetic analogue of the surficial Love number for a charged black hole but it does not prove that the expression is necessarily correct.

It is important to note that there is no literature to compare the full result (given by eq. 4.2.9) to yet. The electromagnetic surficial Love numbers have not been defined or calculated for a Reissner-Nordström black hole, so this is a new result.

4.2.4 Reissner-Nordström black hole - Electromagnetic far-field Love numbers

The calculation of the electromagnetic far-field Love numbers for a Reissner-Nordström black hole is similar to the calculation of the gravitational Love numbers. However, in this case not the first component of the metric but the first component of the perturbation of the electromagnetic potential will be investigated. In analogy to the discussion by Landry and Poisson around [2, equation 2.5] the term growing as $r^l = r^2$ will be compared to the term decaying as $r^{-(l+1)} = r^{-3}$. Considering that an overall factor of r^2 must be pulled out, the term proportional to r^{-5} must be considered, just as in the expansion of the first component of the metric.

Therefore, an expansion in factors of $1/r$ is again relevant. Only taking into account the radial dependence (effectively dividing by $\mathcal{E}^q(\theta,\phi)$) leads to:

$$\begin{aligned}\delta A_0 = -\frac{1}{2}\Bigg[&\frac{4M(C_{1a} - 2C_{1b})}{3Q} - \frac{4M^2C_{1a} + (-8M^2 + Q^2)C_{1b}}{Qr} \\ &- \frac{-8M(M^2+Q^2)C_{1a} + 2M(4M^2+Q^2)C_{1b}}{3Qr^2} - \frac{Q(2M^2C_{1a} + (-4M^2+Q^2)C_{1b}}{r^3} + O\left[\frac{1}{r^6}\right]\Bigg]\end{aligned} \tag{4.2.11}$$

The expansion inside the brackets does not contain a term proportional to $1/r^5$ leading to the conclusion that the quadrupole electromagnetic far-field Love number of the Reissner-Nordström black hole is zero.

4.3 Overview of the results

In this subsection, the results of the calculations of the different Love numbers are summarized. The table below contains the values of the different types of Love numbers that were calculated.

Love number/black hole type	Schwarzschild	Reissner-Nordström
Surficial	$\frac{1}{4}$	$\frac{2C_{1a}-7C_{1b}}{12} - \frac{Q^2 C_{1b}}{16M^2} + O\left[\frac{Q}{M}\right]^3$
Gravitational	0	0
Electromagnetic surficial	NA	$\frac{1}{2} - \frac{3C_2 Q^2}{4M^2(C_1-2C_2)} + O\left[\frac{Q}{M}\right]^3$
Electromagnetic far-field	NA	0

Chapter 5

Conclusion, discussion and outlook

5.1 Conclusion

In this thesis, the perturbations of a Schwarzschild and Reissner-Nordström black hole were investigated. This was done in the Regge-Wheeler as well as light cone gauge, that each place particular restrictions on the components of the metric perturbation. The expressions for these components were found by solving Einstein's (and Maxwell's) equations for these perturbed black holes. These expressions were then used to calculate the quadrupole Love numbers of the two black holes. The results are summarized in table 4.3. Some of the results, particularly the Love numbers for a Schwarzschild black hole, have been obtained before in other literature and the results found here agree with those results. However, there is not any literature on the electromagnetic Love numbers of a Reissner-Nordström black hole, so these results are new.

5.2 Discussion

It has already been mentioned in section 3 that there were some inconsistencies between the perturbations in the Regge-Wheeler gauge and the light cone gauge of Reissner-Nordström black holes. First, in the Regge-Wheeler gauge, a set of three independent solutions was found that each solve Einstein's and Maxwell's equations. For one of these solutions, the one proportional to C_2 which contains log terms, no corresponding solution was found in the light cone gauge. By solving the relevant equations in that gauge, a set of only two independent solutions was obtained, which could also be obtained by applying a gauge transformation from the Regge-Wheeler to the light cone gauge. In section 3.6.1 it was attempted to find an additional solution proportional to C_2 in the light cone gauge but this was unsuccessful. Furthermore, the solution proportional to C_2 that was found for a Reissner-Nordström black hole in the Regge-Wheeler gauge did not have the correct limit $Q \to 0$.

Thus, we have been unable to find a third independent solution, apart from the ones proportional to C_{1a} and C_{1b}, to the Einstein and Maxwell equations for a Reissner-Nordström black hole that has the correct limit $Q \to 0$. Now the question is how big of a problem that is, because if such a solution had been found it might not have been physical. For a Schwarzschild black hole we have seen that the solution proportional to C_2 in either gauge was unphysical since it diverges at $r = 2M$. This is also true in the Reissner-Nordström case in the Regge-Wheeler gauge for the part of the solution proportional to C_2: it diverges at the outer horizon at $r = M + \sqrt{M^2 - Q^2}$. Therefore, we have to set $C_2 = 0$, meaning that this solution is not relevant for calculating the Love numbers. Based on this, we are confident that the solutions that are relevant for calculating the Love numbers have been found.

All other solutions that have been found are consistent: a gauge transformation can be found from the solutions in the Regge-Wheeler gauge to those in the light cone gauge and vice versa. Also, applying the limit $Q \to 0$ to the solutions of the perturbation of the Reissner-Nordström black hole lead to solutions that solved the vacuum Einstein equations of a Schwarzschild black hole. In addition, in the limit $Q \to 0$ the generators of

the gauge transformation for the Reissner-Nordström solutions turned into the generators that transform the Schwarzschild solutions. This makes it all quite probable that the solutions that have been found are correct.

The values of the Love numbers that were calculated in this thesis correspond to those calculated in other literature. For the new Love numbers that have not been calculated before in literature, such a comparison cannot be made. However, when expanding the results for these new Love numbers in terms of Q/M and taking the limit $Q \to 0$, such a comparison can be made. Based on that, we are confident in the results for the Love numbers.

5.3 Outlook

Even though the Reissner-Nordström metric is considerably more complicated than the Schwarzschild metric, it still does not describe a physical black hole, partly because black holes are generally rotating. It is well known that the gravitational Love numbers of non-rotating black holes vanish, while the surficial Love numbers are non-zero. There is a fierce debate what the gravitational Love numbers are for rotating black holes: some research groups advocate that these tidal Love numbers are vanishing [6], [11], while others claim that they are non-zero [12]. It is therefore relevant to calculate the gravitational Love numbers of rotating black holes.

The simplest metric that describes a rotating black hole is the Kerr metric. Despite the fact that a Reissner-Nordström and Kerr black hole are quite different - the former is charged but nonrotating whereas the latter is uncharged but rotating - there is an important similarity between them. Both of these black holes have two horizons, an inner as well as an outer horizon. Therefore, it was relevant to have looked at the Reissner-Nordström black hole whose horizons are spherical, to learn what the effects of two horizons are and if it leads to any conceptual difficulties. Now that we know such difficulties do not arise when dealing with two horizons, similar calculations as have been done in this thesis can be carried out for a Kerr black hole.

However, the two horizons of a Kerr black hole are not spherical, which is one of the reasons why it is more difficult to study them. The equations that result from the same procedure that has been described in this thesis are quite difficult. Therefore, it is useful to use a different formalism to describe a Kerr black hole, one that is not linked to specific coordinates. Two such formalisms are introduced in Appendix B and one is applied in Appendix C.

Appendix A

Full set of equations

A.1 The Regge-Wheeler gauge

A.1.1 Einstein's equations

This section contains the Einstein equations for a Reissner-Nordström black hole in the Regge-Wheeler gauge in Eddington-Finkelstein coordinates. The Einstein and stress-energy tensor each have sixteen components, meaning that there are that same number of Einstein equations. However, many of them are the same and only the nonidentical ones are shown here:

$$0 = (Q^2 + r(-2M+r))((Q^2-4r^2)H_0(r) - 2r^2K(r) + 2Qu_1(r) + (-Q^2r + 2Mr^2 - r^3)\frac{dH_0(r)}{dr} + (2Q^2r - 5Mr^2 + 3r^3)\frac{dK(r)}{dr} - 2Qr\frac{du_1(r)}{dr} + (Q^2r^2 - 2Mr^3 + r^4)\frac{d^2K(r)}{dr^2} \tag{A.1.1}$$

$$0 = \frac{2Q}{r^4}\left(-2ru_2(r) + (Q^2 + r(-2M+r))\frac{du_3(r)}{dr}\right) \tag{A.1.2}$$

$$0 = \frac{1}{r(Q^2+r(-2M+r))}\left(-6rH_0(r) + (Q^2+r(-2M+r))\left(2\frac{dK(r)}{dr} + r\frac{d^2K(r)}{dr^2}\right)\right) \tag{A.1.3}$$

$$0 = \frac{1}{r^2(Q^2+r(-2M+r))}\Bigg(2r(Q^2-Mr)H_0(r) - 4Qru_1(r) + 4Qru_2(r) + (-Q^2r^2 + 2Mr^3 - r^4)\frac{dH_0(r)}{dr} + (Q^2r^2 - 2Mr^3 + r^4)\frac{dK(r)}{dr} + (-2Q^3 + 4MQr - 2Qr^2)\frac{du_3(r)}{dr}\Bigg) \tag{A.1.4}$$

$$0 = \frac{1}{r^2}\Bigg(2Q^2H_0(r) - 4Qu_1(r) + r(-2(Q^2-r^2)\frac{dH_0(r)}{dr} + 2(M-r)r\frac{dK(r)}{dr} + 4Q\frac{du_1(r)}{dr} + (Q^2r - 2Mr^2 + r^3)\frac{d^2H_0(r)}{dr^2} + (-Q^2r + 2Mr^2 - r^3)\frac{d^2K(r)}{dr^2}\Bigg) \tag{A.1.5}$$

A.1.2 Maxwell's equations

$$12ru_1(r) + (Q^2 + r(-2M+r))\left(2Q\frac{dK(r)}{dr} - 2r\frac{d^2u_1(r)}{dr^2}\right) = 0 \tag{A.1.6}$$

$$12r(u_1(r) - u_2(r)) + (Q^2 + r(-2M+r))\left(2Q\frac{dK(r)}{dr} + 6\frac{du_3(r)}{dr} - 2r\frac{d^2u_1(r)}{dr^2}\right) = 0 \tag{A.1.7}$$

$$2ru_2(r) - 2r^2\frac{du_2(r)}{dr} + (-2Q^2 + 2Mr)\frac{du_3(r)}{dr} + (Q^2r - 2Mr^2 + r^3)\frac{d^2u_3(r)}{dr^2} = 0 \tag{A.1.8}$$

The Lorenz gauge condition leads to the equation:

$$QH_1(r) + u_2(r) - 3u_3(r) + Qr\frac{dH_1(r)}{dr} + r\frac{du_2(r)}{dr} = 0 \tag{A.1.9}$$

A.2 Light cone gauge

In this section, the Einstein and Maxwell equations for a perturbed Reissner-Nordström black hole in the light cone gauge are presented in (t, r, θ, ϕ) coordinates.

A.2.1 Einstein's equations

$$0 = \frac{1}{r^6}\Bigg(r^5\frac{de_1(r)}{dr} - 2r^5\frac{de_4(r)}{dr} + 2Qr\frac{du_1(r)}{d}r + 3r^4(Q^2 + 2r(-M+r))e_1(r) \\ - 2r^4(5Q^2 + r(-9M+4r))e_4(r) + (Q^2 + r(-2M+r))(2r^4e_7(r) - 2Qu_1(r))\Bigg) \tag{A.2.1}$$

$$0 = \frac{1}{Q^2 + r(-2M+r)}\Bigg(-r(Q^2 - 2Mr + r^2)\frac{de_4(r)}{dr} + 3r^2e_1(r) + (-5Q^2 + 8Mr - 3r^2)e_4(r)\Bigg) \tag{A.2.2}$$

$$0 = -\frac{1}{3r^4}\Bigg((Q^2r^5 - 2Mr^6 + r^7)\frac{d^2e_4(r)}{dr^2} - 3r^6\frac{de_1(r)}{dr} + (6Q^2r^4 - 12Mr^5 + 6r^6)\frac{de_4(r)}{dr} \\ + (-6Q^3 + 12MQr - 6Qr^2)\frac{du_3(r)}{dr} - 6r^5e_1(r) + 2r^3(2Q^2 - 4Mr + 3r^2)e_4(r) + 12Qru_2(r)\Bigg) \tag{A.2.3}$$

$$0 = \frac{1}{3r^4}\Bigg((Q^2 + r(-2M+r))\left(-r^5\frac{d^2e_4(r)}{dr^2} - 6r^4\frac{de_4(r)}{dr} + 6Q\frac{du_3(r)}{dr}\right) + 3r^6\frac{de_1(r)}{dr} \\ - 12Qru_2(r) + 6r^5e_1(r) + (8Mr^4 - 4Q^2r^3 - 6r^5)e_4(r)\Bigg) \tag{A.2.4}$$

$$0 = \frac{1}{r^2(Q^2 + r(-2M+r))^2}\Bigg(-(Q^2 + r(-2M+r))\left(r^5\frac{de_1(r)}{dr} + 2Qr\frac{du_1(r)}{dr} + 2r^4e_7(r) - 2Qu_1(r)\right) \\ - 3r^4(Q^2 - 2Mr)e_1(r) + 2r^5(-M+r)e_4(r)\Bigg) \tag{A.2.5}$$

$$0 = -\frac{1}{3r(Q^2 + r(-2M+r)}\Bigg(-3r^5\frac{de_1(r)}{dr} + (2Q^2r^3 - 4Mr^4 + 2r^5)\frac{de_7(r)}{dr} \\ - 6r^4e_1(r) + 2r^4e_4(r) + (4Q^2r^2 - 8Mr^3 + 4r^4)e_7(r) + 12Qu_1(r)\Bigg) \tag{A.2.6}$$

$$0 = \frac{1}{6}\Bigg(r(Q^2 - 2Mr + r^2)\frac{d^2e_7(r)}{dr^2} - 2r^2\frac{de_4(r)}{dr} + 2(2Q^2 - 5Mr + 3r^2)\frac{de_7(r)}{dr} \\ + 6r^2e_4(r) - 2(Q^2 + r(-4M+3r))e_7(r)\Bigg) \tag{A.2.7}$$

$$0 = -\frac{1}{r^2}\left(r^6\frac{d^2e_1(r)}{dr^2} + 6r^5\frac{de_1(r)}{dr} - 2r^5\frac{de_4(r)}{dr} - 4Qr\frac{du_1(r)}{dr} + 6r^4e_1(r) - 6r^4e_4(r) + 4Qu1(r)\right) \tag{A.2.8}$$

A.2.2 Maxwell's equations

$$0 = \frac{1}{r^3}\left((Q^2 - 2Mr + r^2)\frac{d^2u_1(r)}{dr^2} - 2Qr^2e_4(r) - 6u_1(r)\right) \tag{A.2.9}$$

$$0 = \frac{1}{r^2(Q^2 + r(-2M+r))}\left(3\left((Q^2 - 2Mr + r^2)\frac{du_3(r)}{dr} - 2ru_2(r)\right) - 2Qr^3e_4(r)\right) \tag{A.2.10}$$

$$0 = -\frac{1}{3r^3}\Bigg((-3Q^2r + 6Mr^2 - 3r^3)\frac{d^2u_3(r)}{dr^2} + 2Qr^4\frac{de_4(r)}{dr} + 6r^2\frac{du_2(r)}{dr} + (6Q^2 - 6Mr)\frac{du_3(r)}{dr} \\ + 2Qr^3e_4(r) - 6ru_2(r)\Bigg) \tag{A.2.11}$$

Appendix B

Tetrad formalism

Although different ones have been used, up until now every equation has been expressed in terms of some coordinates. Transforming to different coordinates affected the equations and some of them were rather complicated and difficult to solve, regardless of which coordinate system was chosen. In this section, two formalisms called the Newman-Penrose (NP) and the Geroch-Held-Penrose (GHP) formalism are introduced. Both of these involve a set of vectors (called tetrad in the case of NP) that are not derived from any coordinate system, meaning that the formalisms are coordinate independent. Furthermore, the relevant equations turn out to be simpler and more compact in these formalisms, especially in the latter one.

Historically, the Newman-Penrose formalism was constructed first and the Geroch-Held-Penrose formalism was essentially an improvement of that, being more efficient. The formalisms are particularly convenient for studying perturbations of the Kerr spacetime since the wave equation describing this is not seperable when written in coordinate language [13]. However, they can also be used to describe the spacetimes that have been discussed in this thesis in a convenient way.

B.1 Newman-Penrose formalism

In the Newman-Penrose formalism a tetrad $e^a_\mu = l^a, n^a, m^a, \overline{m}^a$ is introduced that contains four vectors that form an orthonormal basis. Two of these, l^a and n^a are real null vectors normalized (in case of the mostly minus convention for the metric used here) such that $l_a n^a$ = -1. The other two, m^a and $\overline{m}^a$ are complex, each other's complex conjugate and defined such that $m_a \overline{m}^a = 1$. The following inner products vanish: $l_a l^a$ $= n_a n^a = m_a m^a = \overline{m}_a \overline{m}^a = 0$. Just as one can always perform a coordinate transformation to go to a different coordinate system, the orthonormal basis formed by the tetrad is also not unique. The basis must however remain orthonormal after a transformation, which is ensured by using Lorentz transformations. The indices of the tetrad can be raised and lowered in a similar way to how vector indices are raised and lowered with the spacetime metric:

$$\eta_{\mu\nu} = e^a_\mu e^b_\nu g_{ab}. \tag{B.1.1}$$

The covariant derivative of a tensor with spacetime indices can be written as the sum of a partial derivative term and one or more terms involving Christoffel connections (one for each index) in this way:

$$\nabla_a T^b_c = \partial_a T^b_c + \Gamma^b_{ad} T^d_c - \Gamma^d_{ac} T^b_d. \tag{B.1.2}$$

Similarly, the covariant derivative of a tensor with Lorentz indices involves terms containing spin coefficients $\gamma_{\mu\nu\rho}$[13]:

$$\nabla_\rho T^\mu_\nu = \partial_\rho T^\mu_\nu + \gamma_\rho{}^\mu{}_\lambda T^\lambda_\mu - \gamma_\rho{}^\mu{}_\lambda T^\lambda_\nu. \tag{B.1.3}$$

Just as the Christoffel connections ensure that applying the covariant derivative operator to a tensor forms another tensor, the role of the spin connections is similar. The spin coefficients are defined as [14]:

$$\gamma_{\mu\nu\lambda} = e^a_\mu e^b_\nu \nabla_a e_{\lambda b}, \tag{B.1.4}$$

where metric compatibility implies antisymmetry in the last two indices of $\gamma_{\mu\nu\lambda}$. This difference with the Christoffel connections, which are symmetric under exchange of the last two indices, turns out to be quite profound. It entails a considerably smaller number of degrees of freedom, namely 24 instead of 40. These 24 degrees of freedom are encoded in 12 complex coefficients:

$$\kappa = -\gamma_{(1)(3)(1)} = -l^a m^b \nabla_a l_b \qquad \nu = \gamma_{(2)(4)(2)} = n^a \overline{m}^b \nabla_a n_b \tag{B.1.5a}$$

$$\sigma = -\gamma_{(1)(3)(3)} = -m^a m^b \nabla_a l_b \qquad \lambda = \gamma_{(2)(4)(4)} = \overline{m}^a \overline{m}^b \nabla_a n_b \tag{B.1.5b}$$

$$\rho = -\gamma_{(1)(3)(4)} = -\overline{m}^a m^b \nabla_a l_b \qquad \mu = \gamma_{(2)(4)(3)} = m^a \overline{m}^b \nabla_a n_b \tag{B.1.5c}$$

$$\tau = -\gamma_{(1)(3)(2)} = -n^a m^b \nabla_a l_b \qquad \pi = \gamma_{(2)(4)(1)} = l^a \overline{m}^b \nabla_a l_b \tag{B.1.5d}$$

and

$$\alpha = \frac{1}{2}(\gamma_{(3)(4)(4)} - \gamma_{(1)(2)(4)}) = \frac{1}{2}(\overline{m}^a l^b \nabla_a n_b - \overline{m}^a m^b \nabla_a \overline{m}_b) \tag{B.1.5e}$$

$$\beta = \frac{1}{2}(\gamma_{(3)(4)(3)} - \gamma_{(1)(2)(3)}) = \frac{1}{2}(m^a \overline{m}^b \nabla_a m_b - m^a n^b \nabla_a l_b) \tag{B.1.5f}$$

$$\gamma = \frac{1}{2}(\gamma_{(3)(4)(2)} - \gamma_{(1)(2)(2)}) = \frac{1}{2}(n^a l^b \nabla_a n_b - n^a m^b \nabla_a \overline{m}_b) \tag{B.1.5g}$$

$$\varepsilon = \frac{1}{2}(\gamma_{(3)(4)(1)} - \gamma_{(1)(2)(1)}) = \frac{1}{2}(l^a \overline{m}^b \nabla_a m_b - l^a n^b \nabla_a l_b). \tag{B.1.5h}$$

Furthermore, the tetrad can be used to define directional derivatives:

$$e_\mu = e_\mu^a \frac{\partial}{\partial x^a} \tag{B.1.6}$$

which can be defined individually:

$$D = l^a \frac{\partial}{\partial x^a} \qquad \Delta = n^a \frac{\partial}{\partial x^a} \qquad \delta = m^a \frac{\partial}{\partial x^a} \qquad \overline{\delta} = \overline{m}^a \frac{\partial}{\partial x^a}. \tag{B.1.7}$$

Just as the Riemann tensor can be expressed in terms of the Christoffel symbols, its equivalent in the tetrad formalism can be expressed in terms of the spin coefficients. The Riemann tensor can in general be written in terms of the Weyl tensor C_{abcd}, Ricci tensor R_{ab} and Ricci scalar R (splitting it up into a traceless and trace part respectively):

$$R_{abcd} = C_{abcd} + \frac{1}{2}(g_{ac}R_{bd} + g_{bd}R_{ac} - g_{bc}Rad - g_{ad}R_{bc}) - \frac{1}{2}(g_{ac}g_{bd} - g_{bc}g_{ad})R. \tag{B.1.8}$$

Both the Weyl and the Ricci tensor have ten independent components. In the Newman-Penrose formalism, the ten degrees of freedom of the Weyl tensor are contained in five complex scalars Ψ_i:

$$\Psi_0 = C_{abcd} l^a m^b l^c m^d \tag{B.1.9a}$$

$$\Psi_1 = C_{abcd} l^a n^b l^c m^d \tag{B.1.9b}$$

$$\Psi_2 = \frac{1}{2} C_{abcd}(l^a n^b l^c n^d - l^a n^b m^c \overline{m}^d) \tag{B.1.9c}$$

$$\Psi_3 = C_{abcd} l^a n^b \overline{m}^c n^d \tag{B.1.9d}$$

$$\Psi_4 = C_{abcd} n^a \overline{m}^b n^c \overline{m}^d. \tag{B.1.9e}$$

The ten degrees of freedom of the Ricci tensor are captured in ten (real) scalars:

$$\Phi_{00} = -\frac{1}{2}R_{11} \qquad \Phi_{21} = -\frac{1}{2}R_{24} \tag{B.1.10}$$

$$\Phi_{11} = -\frac{1}{4}(R_{12} + R_{34}) \qquad \Phi_{02} = -\frac{1}{2}R_{33} \tag{B.1.11}$$

$$\Phi_{01} = -\frac{1}{2}R_{13} \qquad \Phi_{22} = -\frac{1}{2}R_{22} \tag{B.1.12}$$

$$\Phi_{12} = -\frac{1}{2}R_{23} \qquad \Phi_{20} = -\frac{1}{2}R_{44} \tag{B.1.13}$$

$$\Phi_{10} = -\frac{1}{2}R_{14} \qquad \Pi = \frac{1}{24}R. \tag{B.1.14}$$

All these quantities can be used to describe spacetime as a vacuum, e.g. to describe neutral black holes [15]. To describe parts of spacetime that are not a vacuum (such as charged black holes), the tetrad components of the electromagnetic field tensor must be included [16]:

$$\Phi_0 = F_{ab} l^a m^b \qquad \Phi_1 = \frac{1}{2} F_{ab}(l^a n^b + \overline{m}^a m^b) \qquad \Phi_2 = F_{ab} \overline{m}^a n^b. \tag{B.1.15}$$

With the reduced number of degrees of freedom and parameters, the efficiency of the NP formalism is quite clear. However, the GHP formalism will turn out to be even more efficient.

B.2 Geroch-Held-Penrose formalism

The Geroch-Held-Penrose (GHP) formalism follows from the Newman-Penrose formalism by introducing some modifications. First of all, the prime (') operation is introduced, which has the following effect on the vectors in the tetrad:

$$(l^a)' = n^a, \qquad (n^a)' = l^a, \qquad (m^a)' = \overline{m}^a, \qquad (\overline{m}^a)' = m^a. \tag{B.2.1}$$

Using this prime operation, six of the spin coefficients can be written in terms of the others and as such are not independent anymore:

$$\kappa' = -\nu, \qquad \sigma' = -\lambda, \qquad \rho' = -\mu, \qquad \tau' = -\pi, \qquad \beta' = -\alpha, \qquad \varepsilon' = -\gamma. \tag{B.2.2}$$

From this, one of the advantages of the GHP formalism immediately becomes apparent, which is that it reduces (halves) the number of independent spin coefficients. The number of independent directional derivatives is also halved by relating two of them to the other two in the following way: $D' = \Delta$ and $\delta' = \overline{\delta}$.

The number of independent Weyl scalars is also reduced by the following correspondences:

$$\Psi_4 = \Psi_0', \qquad \Psi_3 = \Psi_1'. \tag{B.2.3}$$

Hence, in the GHP formalism there are only three independent Weyl scalars, as opposed to five in the NP formalism. Similarly for the Ricci scalars:

$$\Phi_{12} = \Phi_{10}', \qquad \Phi_{20} = \Phi_{02}', \qquad \Phi_{21} = \Phi_{01}', \qquad \Phi_{22} = \Phi_{00}'. \tag{B.2.4}$$

Thus, in the GHP formalism there are four fewer (five instead of nine) independent Ricci scalars than in the NP formalism [17].

B.2.1 Lorentz transformations

As stated before, the orthonormal basis formed by the tetrad vectors is not unique. A Lorentz transformation can be applied that will transform (some of) the vectors whilst preserving their orthonormality and normalization. These transformations can be split up into three classes that each have a different effect on the NP and GHP quantities:

- Rotations of class I which leave l unchanged and change the other vectors in the following way: $m \to m + al$, $\overline{m} \to \overline{m} + a^* l$ and $n \to n + a^* m + a\overline{m} + aa^* l$.
- Rotations of class II that leave n unchanged and have the following effect on the other vectors: $m \to m + bn$, $\overline{m} \to \overline{m} + b^* n$ and $l \to l + b^* m + b\overline{m} + bb^* n$.
- Rotations of class III that leave the direction of both l and n unchanged but can change their magnitude: $l \to A^{-1} l$, $n \to An$, and rotate the other two vectors: $m \to e^{iB} m$ and $\overline{m} \to e^{-iB} \overline{m}$.

In these transformations, a and b are complex functions and A and B are real ones [18]. We will now use the third class of rotations to define the GHP type.

B.2.2 Dimensional analysis

Dimensional analysis is a very useful tool, especially in physics, to check outcomes of calculations. If the dimensions on both sides of an equation match, it is much more likely that the calculations have been done correctly. A similar technique can be used in the GHP formalism, by exploiting the fact that every important object in this formalism has a GHP type. The GHP type of an object is determined by how it transforms under a particular type of Lorentz transformations, a rotation of class III. The effect of such a rotation, the rescaling of the real vectors and rotating of the complex vectors can be combined into one transformation by defining $\lambda = Ae^{iB}$. The transformation of any tensorial object can then be written as: $\lambda^p \overline{\lambda}^q$ for an object of type $\{p, q\}$ [13].

To be able to compare the GHP type of objects to check equations, the type of each object must be well-defined. Acting any of the directional derivatives defined in section B.1 on a scalar χ of type $\{p, q\}$ does not produce an object with a well defined GHP type. However, two new operators, "thorn" and "edth" can be defined that do produce objects with a well-defined type when applied to a scalar:

$$\text{þ}\,\chi = [D - p\varepsilon - q\overline{\varepsilon}]\chi \qquad\qquad \text{ð}\,\chi = [\delta - p\beta + q\overline{\beta}']\chi \tag{B.2.5}$$

These operators also have a primed version:

$$\text{þ}'\,\chi = [D' + p\varepsilon' + q\overline{\varepsilon}']\chi \qquad\qquad \text{ð}'\,\chi = [\delta' + p\beta' - q\overline{\beta}]\chi. \tag{B.2.6}$$

These four derivative operators, thorn, edth and their primed versions can be combined to form a covariant derivative operator:

$$\Theta_a = l_a\,\text{þ}' + n_a\,\text{þ} - m_a\,\text{ð}' - \overline{m}_a\,\text{ð} \tag{B.2.7}$$

Just like moving from classical physics to General Relativity by replacing every partial derivative ∂_μ by the covariant derivative D_μ, moving from GR in coordinate language to GHP language can be done by exchanging D_μ by Θ_μ [15].

B.2.3 Important equations and properties

For any type-D spacetime (which all spacetimes considered here are), the Goldberg-Sachs theorem implies:

$$\kappa = \kappa' = \sigma = \sigma' = 0. \tag{B.2.8}$$

Furthermore, four of the Weyl scalars obey:

$$\Psi_0 = \Psi_1 = \Psi_3 = \Psi_4 = 0. \tag{B.2.9}$$

This holds irrespective of the chosen tetrad, with the only restriction that l^a and n^a must be aligned with the principle null directions. These equations will be checked for a specific tetrad in upcoming sections.

An important equation in the tetrad formalism is the Teukolsky equation. It governs how gravitational waves propagate on a (Kerr) spacetime with no sources [13]. For a part of the derivation of the Teukolsky equation, which will not be presented here, linear perturbation theory is used such that for example Ψ_0 can be written as: $\Psi_0 = \Psi_0^{(0)} + \Psi_0^{(1)}$. The Teukolsky equation will then be like a wave equation for $\Psi_0^{(1)}$, the linear perturbation term of Ψ_0. The Teukolsky equation is generally written in terms of the operators just defined:

$$(\text{þ}\,\text{þ}' - \text{ð}\,\text{ð}' - \rho'\,\text{þ} - (4\rho + \overline{\rho})\,\text{þ}' + \tau'\,\text{ð} + (4\tau + \overline{\tau}'\,\text{ð}' + 4\rho\rho' - 4\tau\tau' - 2\Psi_2)\Psi_0^{(1)} = 0. \tag{B.2.10}$$

B.2.4 Kerr black hole

A spinning black hole is described by the Kerr metric whose line-element is conveniently written in terms of Boyer-Lindquist coordinates (t, r, θ, ϕ):

$$ds^2 = -\left[1 - \frac{2Mr}{\Sigma}\right] dt^2 - \frac{4aMr\sin^2\theta}{\Sigma} dt d\phi + \frac{\Sigma}{\Delta} dr^2 + \Sigma d\theta^2 + \left[\Delta + \frac{2Mr(r^2+a^2)}{\Sigma}\right] \sin^2\theta d\phi^2. \quad \text{(B.2.11)}$$

Here, a is the angular momentum per unit mass of the rotating black hole, $\Sigma = r^2 + a^2\cos^2\theta$ and $\Delta = r^2 - 2Mr + a^2$.

The Teukolsky equations in these coordinates is:

$$\begin{aligned} 0 = &\left[\frac{(r^2+a^2)^2}{\Delta} - a^2\sin^2\theta\right] \frac{\partial^2}{\partial t^2}\Psi_0^{(1)} + \frac{4Mar}{\Delta}\frac{\partial^2}{\partial t \partial\phi}\Psi_0^{(1)} + \left[\frac{a^2}{\Delta} - \frac{1}{\sin^2\theta}\right]\frac{\partial^2}{\partial^2\phi}\Psi_0^{(1)} \\ &- \Delta^{-s}\frac{\partial}{\partial r}\left(\Delta^{s+1}\frac{\partial}{\partial r}\Psi_0^{(1)}\right) - \frac{1}{\sin\theta}\frac{\partial}{\partial\theta}\left(\sin\theta\frac{\partial}{\partial\theta}\right) - 2s\left[\frac{a(r-M)}{\Delta} + i\frac{\cos\theta}{\sin^2\theta}\right]\frac{\partial}{\partial\phi}\Psi_0^{(1)} \\ &- 2s\left[\frac{M(r^2-a^2)}{\Delta} - r - ia\cos\theta\right]\frac{\partial}{\partial t}\Psi_0^{(1)} + \left[s^2\cot^2\theta - s\right]\Psi_0^{(1)}, \end{aligned} \quad \text{(B.2.12)}$$

where s is the "spin weight" that characterizes the type of perturbation: $s = 0$ for scalar, $s = 1$ for electromagnetic and $s = 2$ for gravitational perturbations. Particularly remarkable about this equation is that it is seperable, the time dependence, radial dependence and angular dependence can be separated from each other [13].

Appendix C

Applying the formalism

In this section, the formalisms that have just been introduced will be applied to the Reissner-Nordström and Schwarzschild metric, where the latter will again follow from taking the limit $Q \to 0$ in the former. As a matter of fact, the procedure for both metrics is identical and when the equations are expressed in terms of f they look the same, only f will differ. It will be shown that it does not matter which coordinate system is used, nor does it matter in which gauge the procedure is carried out, the equations will be the same regardless.

C.1 Some calculations

In this section, it is shown how some calculations in the tetrad formalism proceed by means of a specific example.

C.1.1 Construction of a specific tetrad

First, it is shown how a tetrad can be constructed from the metric. For this, the line-element in Eddington-Finkelstein coordinates is a natural starting point: $ds^2 = -fdv^2 + 2dvdr + r^2(d\theta^2 + \sin^2\theta d\phi^2)$. To construct the vectors l^a and n^a, radial geodesics will be investigated, meaning $d\theta = d\phi = 0$ and thus we are left with: $ds^2 = -fdv^2 + 2dvdr$. Looking at radial null geodesics implies: $0 = ds^2 = -fdv^2 + 2dvdr$ which has an outgoing solution; $-fdv + 2dr = 0$ and an ingoing solution; $dv = 0$. From these, the vectors l^a and n^a can be constructed, respectively:

$$l^a = (1, \frac{f}{2}, 0, 0), \qquad n^a = (0, -1, 0, 0). \tag{C.1.1}$$

Using the Schwarzschild metric to lower an index of one of the vectors; $n_a = g_{ab}n^b = (-1, 0, 0, 0)$ leads to; $l^a n_a = -1$. This is in agreement with the normalization as it was defined in the mostly-plus convention.

The complex null-vector m^a must be orthogonal to the other two and will therefore be constructed from a θ- and ϕ-component only. The latter component will be complex to ensure that m^a is complex, so that we have: $m^a = (0, 0, A, iB)$ and $\overline{m}^a = (0, 0, A, -iB)$. From the normalization $m^a m_a = 0$ it follows that $B = A/\sin\theta$ and $m^a\overline{m}_a = 1$ leads to $A = 1/(\sqrt{2}r)$. Thus, the complex null-vectors of the NP formalism are:

$$m^a = \frac{1}{\sqrt{2}r}(0, 0, 1, \frac{i}{\sin\theta}), \qquad \overline{m}^a = \frac{1}{\sqrt{2}r}(0, 0, 1, \frac{-i}{\sin\theta}). \tag{C.1.2}$$

This example is particularly instructive to show how a tetrad can be constructed, but this one will not be used for any calculations. For that, a more widely used tetrad called the Kinnersly tetrad will be used which will not be derived.

C.1.2 Calculating the spin coefficients

For the complex spin coefficients, a few will be calculated as an example and the others will simply be stated. As a first example, take κ for which we know: $\kappa = l^a m^b \nabla_a l_b$. This requires no calculation, since it can immediately be concluded from the orthogonality of l^a and m^a that $\kappa = 0$. A non-zero coefficient is ρ, which can be evaluated from; $\rho = \overline{m}^a m^b \nabla_a l_b$. In this formalism, repeated indices are still summed over, thus we have:

$$\begin{aligned}
\rho &= \overline{m}^a m^b (\partial_a l_b - \Gamma^c{}_{ab} l_c) \\
&= \frac{1}{\sqrt{2}r} m^b \left(\partial_\theta l_b - \Gamma^c{}_{\theta b} l_c - \frac{i}{\sin\theta} (\partial_\phi l_b - \Gamma^c{}_{\phi b} l_c) \right) \\
&= \frac{1}{2r^2} \left(-\Gamma^c{}_{\theta\theta} l_c + \frac{i}{\sin\theta} (-\Gamma^c{}_{\theta\phi} l_c) \right) - \frac{i}{2r^2 \sin\theta} \left(-\Gamma^c{}_{\phi\theta} l_c + \frac{i}{\sin\theta} (-\Gamma^c{}_{\phi\phi} l_c) \right) \\
&= \frac{1}{2r^2} \left(-(-r) \cdot \frac{-f}{2} \right) - \frac{i}{2r^2 \sin\theta} \cdot \frac{i}{\sin\theta} \left(-(-r \sin^2\theta) \cdot \frac{-f}{2} - (-fr \sin^2\theta) \right) \\
&= -\frac{1}{2r} f. \qquad \text{(C.1.3)}
\end{aligned}$$

Calculating the other spin coefficients proceeds in a similar way and the results will simply be given here. Many of the spin coefficients are zero: $\kappa = \sigma = \tau = \nu = \lambda = \pi = \gamma = 0$. The non-zero spin coefficients except ρ that was calculated above are:

$$\alpha = -\beta = \frac{\cot\theta}{2\sqrt{2}r}, \qquad \varepsilon = \frac{M}{2r^2}, \qquad \mu = -\frac{1}{r}. \qquad \text{(C.1.4)}$$

.

There is, as expected, only one nonzero Weyl scalar: $\Psi_2 = -\frac{M}{r^3}$ and all Ricci scalars are zero. All calculations of the quantities listed here can be done for different tetrads and each should yield the same results, regardless of the tetrad.

C.2 Charged black holes

C.2.1 The background

For the Kerr spacetime in (t, r, θ, ϕ)-coordinates, the Kinnersley tetrad is a common one [16]. To move from Kerr to the spacetime under consideration for this thesis, we have to set $a = 0$. Then, the Kinnersley tetrad becomes:

$$l^a = (\frac{1}{f}, 1, 0, 0), \qquad n^a = (1, -f, 0, 0), \qquad m^a = \frac{1}{\sqrt{2}r}(0, 0, 1, \frac{i}{\sin\theta}). \qquad \text{(C.2.1)}$$

To find the tetrad in Eddington-Finkelstein coordinates, one can perform a coordinate transformation. Using $dv = dt$ and $dr = f^{-1}dv + dr$, the following tetrad is obtained:

$$l^a = (\frac{2}{f}, 1, 0, 0), \qquad n^a = (0, -\frac{f}{2}, 0, 0), \qquad m^a = \frac{1}{\sqrt{2}r}(0, 0, 1, \frac{i}{\sin\theta}). \qquad \text{(C.2.2)}$$

These tetrads will be used for calculations in the upcoming sections.

C.2.2 Including perturbations

Besides the freedom to choose a coordinates system when constructing the tetrad vectors, an additional freedom arises when perturbations are included. In that case, there is namely also the gauge freedom that arises. We will use Eddington-Finkelstein coordinates to write the perturbed tetrad vectors in different gauges. Hence, the tetrad given by eq. (C.2.2) will be used as background. The procedure for finding the perturbed real vectors l^a and n^a is then to add perturbation vectors to the background ones:

$$l^a = (\frac{2}{f}, 1, 0, 0) + (a\varepsilon, b\varepsilon, 0, 0) \qquad n^a = (0, -\frac{f}{2}, 0, 0) + (c\varepsilon, d\varepsilon, 0, 0), \qquad \text{(C.2.3)}$$

where a, b, c and d are real parameters.

For the complex vectors m^a and $\overline{m}^a$ the procedure is similar:

$$m^a = \frac{1}{\sqrt{2}r}(0,0,1,\frac{i}{\sin\theta}) + (0,0,\varepsilon(p+iq),\varepsilon(r+is))$$
$$\overline{m}^a = \frac{1}{\sqrt{2}r}(0,0,1,\frac{-i}{\sin\theta}) + (0,0,\varepsilon(p-iq),\varepsilon(r-is)), \tag{C.2.4}$$

where p, q, r and s are again real parameters but not the same ones as before.

The free parameters can be determined from some conditions. The restrictions on a, b, c and d arise from the conditions: $l^a l_a = n^a n_a = 0$ and $l^a n_a = -1$. These three conditions fix three of the four parameters, the fourth one remains undetermined. The p, q, r and s are found by demanding that the norm of m^a and $\overline{m}^a$ is 0 and the inner product of the two vectors 1. This again fixed three parameters, leaving one free parameter.

C.2.3 The light cone gauge

In the light cone gauge, the functions $e_1(r)$, $e_4(r)$ and $e_7(r)$ that we have encountered before will appear in the the perturbed metric. Since the metric is used to calculate inner products, e.g. $l^a n_a = g_{ab} l^a n^b$, the functions will also appear in the perturbed tetrad vectors. The following expressions are found for a, b, c and d:

$$b = \frac{r^2 e_1(r)}{f}\mathcal{E}^q(\theta,\phi) + \frac{a}{2}f \qquad c = 0 \qquad d = \frac{a}{4}f^2. \tag{C.2.5}$$

Where three of the parameters are expressed in terms of the fourth one which is free. Plugging these values into the vectors gives the desired results, regardless of the value of a (it simply does not appear in the expressions): $m^a m_a = \overline{m}^a \overline{m}_a = 0$ and $m^a \overline{m}_a = \overline{m}^a m_a = 1$.

The solutions for the parameters p, q, x and y that appear in the complex vectors are:

$$p = \frac{re_7(r)}{6\sqrt{2}}\mathcal{E}^q_{\theta\theta}(\theta,\phi) \qquad q = -x\sin\theta + \frac{re_7(r)}{3\sqrt{2}}\frac{\mathcal{E}^q_{\theta\phi}(\theta,\phi)}{\sin\theta} \qquad y = \frac{re_7(r)}{6\sqrt{2}}\frac{\mathcal{E}^q_{\phi\phi}(\theta,\phi)}{\sin^3\theta}, \tag{C.2.6}$$

where x is now a free parameter.

C.2.4 The Regge-Wheeler gauge

Due to the coordinate invariant nature of the NP and GHP formalisms, for a particular metric the spin coefficients and the Weyl and Ricci scalars are gauge invariant. Specifically, the quantities that follow from the tetrad in the light cone gauge must be the same as the quantities that follow from the tetrad in the Regge-Wheeler gauge. This will be checked for some of the quantities in this section, leaving the remaining ones to the reader.

In the Regge-Wheeler gauge, the functions $H_0(r)$ and $K(r)$ from the metric perturbation will appear in the vectors of the tetrad. For the real as well as the complex vectors of the tetrad, the procedure for determining them is the same as in the light cone gauge. The parameters of the real vectors are:

$$b = -\frac{H_0(r)}{2}\mathcal{E}^q(\theta,\phi) + \frac{a}{2}f \qquad c = \frac{H_0(r)}{2}\mathcal{E}^q(\theta,\phi) \qquad d = \frac{a}{4}f^2 + \frac{H_0(r)}{2}\mathcal{E}^q(\theta,\phi), \tag{C.2.7}$$

with again a as a free parameter.

The values for the parameters p, q, x and y of the complex vectors are now:

$$p = -\frac{K(r)}{2\sqrt{2}r}\mathcal{E}^q(\theta,\phi) \qquad q = x = 0, \qquad y = -\frac{K(r)}{2\sqrt{2}r}\frac{\mathcal{E}^q(\theta,\phi)}{\sin\theta}. \tag{C.2.8}$$

C.2.5 The GHP formalism for the Schwarzschild metric

The same spin coefficients and scalars that were calculated in the light cone gauge will be calculated here, in order to compare them. The Weyl scalar can again be split up (to first order) as: $\Psi_0 = \Psi_0^{(0)} + \Psi_0^{(1)}\varepsilon$, where again $\Psi_0^{(0)} = 0$ since the background metric is identical for both gauges. The first order, perturbed part looks different:

$$\Psi_0^{(1)} = -\frac{fH_0(r)}{8r^2}\left(-2i\frac{\partial_\phi \mathcal{E}^q(\theta,\phi)}{\sin\theta\tan\theta} - \frac{\partial_\phi^2 \mathcal{E}^q(\theta,\phi)}{\sin^2\theta} - \frac{\partial_\theta \mathcal{E}^q(\theta,\phi)}{\tan\theta} + 2i\frac{\partial_\theta\partial_\phi \mathcal{E}^q(\theta,\phi)}{\sin\theta} + \partial_\theta^2 \mathcal{E}^q(\theta,\phi)\right) \tag{C.2.9}$$

C.2.6 Coordinate transformation

Whereas the construction of a specific tetrad involves choosing a particular coordinate system, all quantities that are defined in terms of the tetrad vectors are coordinate independent by construction. This means that executing the same procedure as in the previous sections, with a tetrad that is constructed in a different coordinate system, all resulting quantities should have the same value.

C.2.7 Application

The tetrad and spin coefficients calculated above can be applied to the equations in [19]. For each of the equations that was considered, the left-hand side was calculated by plugging in the tetrad and spin coefficients that were calculated. The same was done for the right-hand side and then the results were subtracted from each other. The expressions on either side then involved the functions $e_1(r)$, $e_4(r)$ and $e_7(r)$ or $H_0(r)$ and $K(r)$, depending in the gauge. When the expressions that were found in chapter 3 were subsequently plugged in, this yielded zero for all of the equations that were considered. With these additional checks, we can be more confident about the results that have been obtained for the metric perturbation.

Bibliography

[1] K. Martel and E. Poisson, "Gravitational perturbations of the Schwarzschild spacetime: A Practical covariant and gauge-invariant formalism," *Phys. Rev. D*, vol. 71, p. 104003, 2005.

[2] P. Landry and E. Poisson, "Relativistic theory of surficial Love numbers," *Phys. Rev. D*, vol. 89, no. 12, p. 124011, 2014.

[3] B. Preston and E. Poisson, "A light-cone gauge for black-hole perturbation theory," *Phys. Rev. D*, vol. 74, p. 064010, 2006.

[4] R. S. Massey, "Tidal deformations of a Schwarzschild black hole," July 2016.

[5] T. Binnington and E. Poisson, "Relativistic theory of tidal Love numbers," *Phys. Rev. D*, vol. 80, p. 084018, 2009.

[6] A. Le Tiec, M. Casals, and E. Franzin, "Tidal Love Numbers of Kerr Black Holes," 10 2020.

[7] T. Hinderer, "Tidal Love numbers of neutron stars," *Astrophys. J.*, vol. 677, pp. 1216–1220, 2008.

[8] T. Damour and O. M. Lecian, "On the gravitational polarizability of black holes," *Phys. Rev. D*, vol. 80, p. 044017, 2009.

[9] E. Poisson, "Metric of a tidally distorted, nonrotating black hole," *Phys. Rev. Lett.*, vol. 94, p. 161103, 2005.

[10] P. Pani, L. Gualtieri, A. Maselli, and V. Ferrari, "Tidal deformations of a spinning compact object," *Phys. Rev. D*, vol. 92, no. 2, p. 024010, 2015.

[11] A. Le Tiec and M. Casals, "Spinning Black Holes Fall in Love," *Phys. Rev. Lett.*, vol. 126, no. 13, p. 131102, 2021.

[12] H. S. Chia, "Tidal deformation and dissipation of rotating black holes," *Phys. Rev. D*, vol. 104, no. 2, p. 024013, 2021.

[13] B. Bonga, "Foundations of gravitational waves and black hole perturbation theory," 2021.

[14] E. Newman and R. Penrose, "An Approach to gravitational radiation by a method of spin coefficients," *J. Math. Phys.*, vol. 3, pp. 566–578, 1962.

[15] L. R. Price, *Developments in the perturbation theory of algebraically special spacetimes.* PhD thesis, University of Florida, Jan. 2007.

[16] S. K. Bose, "Studies in the kerrnewman metric," *Journal of Mathematical Physics*, vol. 16, no. 4, pp. 772–775, 1975.

[17] R. P. Geroch, A. Held, and R. Penrose, "A space-time calculus based on pairs of null directions," *J. Math. Phys.*, vol. 14, pp. 874–881, 1973.

[18] S. Chandrasekhar, *The mathematical theory of black holes.* 1985.

[19] B. Krishnan, "The spacetime in the neighborhood of a general isolated black hole," *Class. Quant. Grav.*, vol. 29, p. 205006, 2012.